Türkiye Jeoloji Bülteni
Geological Bulletin of Turkey
69 (2026) 45-72
doi: 10.25288/tjb.1764368

The Biruni Fault of the Anatolian Diagonal: Morphological, Seismological and Seismic Reflection Data and Implications for the Neotectonic Framework of the Eastern Mediterranean

Anadolu Çaprazı'na ait Biruni Fayı: Morfolojik, Sismolojik ve Sismik Yansıma Verileri ile Doğu Akdeniz'in Neotektonik Çerçevesi Üzerindeki Etkileri

Nuray Şahbaz[1,2], Esra Tunçel[3], Bülent Kaypak[4], Gürol Seyitoğlu[2]

[1] *Mediterranean Project, Exploration Department, Turkish Petroleum Corporation, Ankara, Türkiye*
[2] *Department of Geological Engineering, Tectonics Research Group, Ankara University, Ankara, Türkiye*
[3] *Department of Geography, Bilecik Şeyh Edebali University, Bilecik, Türkiye*
[4] *Department of Geophysical Engineering, Ankara University, Ankara, Türkiye*

• Geliş/Received: 17.8.2025 • Düzeltilmiş Metin Geliş/Revised Manuscript Received: 19.9.2025 • Kabul/Accepted: 23.09.2025
• Çevrimiçi Yayın/Available online: 03.11.2025 • Baskı/Printed: 31.01.2026

Research Article/Araştırma Makalesi *Türkiye Jeol. Bül. / Geol. Bull. Turkey*

Abstract: The Anatolian Diagonal is a prominent left-lateral shear zone that plays a key role in the neotectonic framework of Türkiye, spanning 170 km between the Central Anatolian and East Anatolian fault zones and extending approximately 850 km from Erzincan to the Cyprus Arc. Its southwestern onshore termination is represented by the Ecemiş-Deliler Fault, while its offshore continuation, the Biruni Fault, trends toward the Cyprus Arc. This study aims to characterise the southwestern end of the Ecemiş-Deliler Fault through geomorphic markers, and to identify the Biruni Fault using key offshore seismic reflection profiles and geological cross-sections provided by Turkish Petroleum. Focal mechanism solutions for offshore seismic events are also examined to assess fault kinematics. Based on onshore observations, a left-lateral offset of 18 km along the Göksu River indicates a long-term slip rate of approximately 2.25 mm/year at the southwestern end of the Ecemiş-Deliler Fault. Offshore, detailed definition and mapping of the Biruni Fault revealed that it comprises a zone of closely spaced, parallel strike-slip segments in its northeastern sector, transitioning into a single linear fault trace that extends south westward toward the Aegean Arc. Despite its clear morphological expression, the southwest end of Ecemiş-Deliler fault and the Biruni Fault of the Anatolian Diagonal have low seismic activity, likely because most regional deformation is accommodated further west along the Antalya-Kekova Fault Zone and the Ptolemy–Pliny–Strabo Fault Zone. The restraining stepovers of the Antalya Thrust and Fethiye Thrust between these structures provide new insight into a slip partitioning in the eastern Mediterranean.

Keywords: Anatolian Diagonal, Biruni Fault, Eastern Mediterranean, Ecemiş-Deliler Fault Zone, morphotectonics, neotectonics

Öz: *Anadolu Çaprazı, Türkiye'nin neotektonik yapısında önemli bir rol oynayan, Orta Anadolu ve Doğu Anadolu fay zonları arasında 170 km ve Erzincan'dan Kıbrıs Yayına kadar yaklaşık 850 km uzanan belirgin bir sol yanal makaslama zonudur. Güneybatıda karadaki ucu Ecemiş-Deliler Fayı ile temsil edilirken, açık denizdeki devamı olan Biruni Fayı, Kıbrıs Yayına doğru yönelmektedir. Bu çalışma, Ecemiş-Deliler Fayı'nın güneybatı ucunu jeomorfolojik belirteçler aracılığıyla karakterize etmeyi ve Türkiye Petrolleri tarafından sağlanan önemli açık deniz sismik yansıma profilleri ve jeolojik kesitler kullanarak Biruni Fayı'nı tanımlamayı amaçlamaktadır. Ayrıca, fay kinematiğini değerlendirmek için açık deniz sismik olaylarının odak mekanizması çözümleri de incelenmiştir. Kara*

* Correspondence / *Yazışma:* nsahbaz@tpao.gov.tr

gözlemlerine göre, Göksu Nehri boyunca 18 km'lik sol yanal ötelenme, Ecemiş-Deliler Fayı'nın güneybatı ucunda yılda yaklaşık 2,25 mm'lik uzun vadeli bir kayma hızına işaret etmektedir. Açık denizde, Biruni Fayı'nın ayrıntılı bir şekilde tanımlanması ve haritalaması ile fayın kuzeydoğu kesiminde birbirine yakın, paralel doğrultu atımlı segmentlerden oluşan bir zondan oluştuğunu ve güneybatıya, Ege Yayına doğru uzanan tek bir doğrusal fay izine dönüştüğünü ortaya koymuştur. Açık morfolojik ifadesine rağmen, Anadolu Çaprazı'ndaki Ecemiş-Deliler Fayı'nın güneybatı ucu ile Biruni Fayı düşük sismik aktivite göstermektedir. Bunun nedeni, bölgesel deformasyonun çoğunun daha batıdaki Antalya-Kekova Fay Zonu ve Ptolemy-Plinius-Strabo Fay Zonu boyunca karşılanması olabilir. Bu yapılar arasında gelişen Antalya Bindirmesi ve Fethiye Bindirmesi, Doğu Akdeniz'deki kayma bölümlenmesine yeni bir bakış açısı sağlamaktadır.

Anahtar Kelimeler: *Anadolu Çaprazı, Biruni Fayı, Doğu Akdeniz, Ecemiş-Deliler Fay Zonu, morfotektonik, neotektonik.*

INTRODUCTION

When explaining the fundamental principles of the neotectonics of Türkiye, it was stated that the main role in the westward escape of the Anatolian Plate was undertaken by the North Anatolian Fault Zone (NAFZ) and the East Anatolian Fault Zone (EAFZ) (Şengör, 1980; Şengör et al., 1985) (Figure 1). The Ecemiş Fault was recognised as an important fault line within the Anatolian Plate and shown on neotectonic maps (Şengör et al., 1985; Şaroğlu et al., 1992), though activity in the pre-neotectonic period was also documented (Yetiş, 1978; Jaffey and Robertson, 2001). Later studies defined the Ecemiş Fault as part of a regionwide structure, the Central Anatolian Fault Zone (Koçyiğit and Beyhan, 1998). In the evaluation of the Central Anatolian Fault Zone (Koçyiğit and Beyhan, 1998; Dirik, 2001; İnan and Ekingen, 2007), an important inadequacy is the lack of a clear relationship with the Cyprus Arc, probably due to limited earlier studies dealing with the structures between Anatolia and Cyprus (Anastasakis and Kelling, 1991; Evans et al., 1978). Therefore, the relationship between the Central Anatolian Fault Zone and the Cyprus Arc remains an unsolved problem.

With an increase in offshore seismic reflection studies, the left-lateral strike-slip Kozan Fault was identified and evaluated as a splay detaching from the EAFZ (Aksu et al., 2014a, b). Based on the identification of normal faults with different directions on seismic reflection sections within the Kozan Fault zone and not being able to explain their directions within the left-lateral system, Aksu et al. (2014b) interpreted some of the normal faults as gravity structures. Moreover, the migration of the Göksu Delta to the southwest over time was explained by the existence of the Kozan Fault zone, and the slip on the fault was stated to be between 6-10 mm/yr (Aksu et al., 2014b).

In a recent paper, Aksu et al. (2022) suggested that right- and left-lateral strike-slip faults come together between the Anamur (Anatolia) - Koruçam / Kormakiti (Cyprus) capes and form the Anamur-Kormakiti (Koruçam) zone. This generally displays as positive flower structures, and the authors concluded that connecting the Central Anatolian Fault Zone to the Cyprus Arc, as implied in previous studies, is impossible.

However, Seyitoğlu et al. (2022a) redefined the Central Anatolian Fault Zone as the northwest margin of the Anatolian Diagonal, a broad left-lateral shear zone (Figure 1). In this redefinition, the Central Anatolian Fault Zone is separated from the NAFZ by the Karaca and Kemah-İliç Faults. They created a restraining bend, the Divriği Thrust, with the Ecemiş-Deliler Fault. The offshore continuation of the Ecemiş-Deliler Fault (EDF), the Biruni Fault, extends to the Cyprus Arc, as recognised by re-evaluating seismic reflection data mainly published by Mansfield (2005) (Figure 1). Global Navigation Satellite Systems (GNSS) based block modelling reveals left-lateral slip rates ranging from 11.7 to 4.2 mm/yr along the Biruni Fault (Seyitoğlu et al., 2022b).

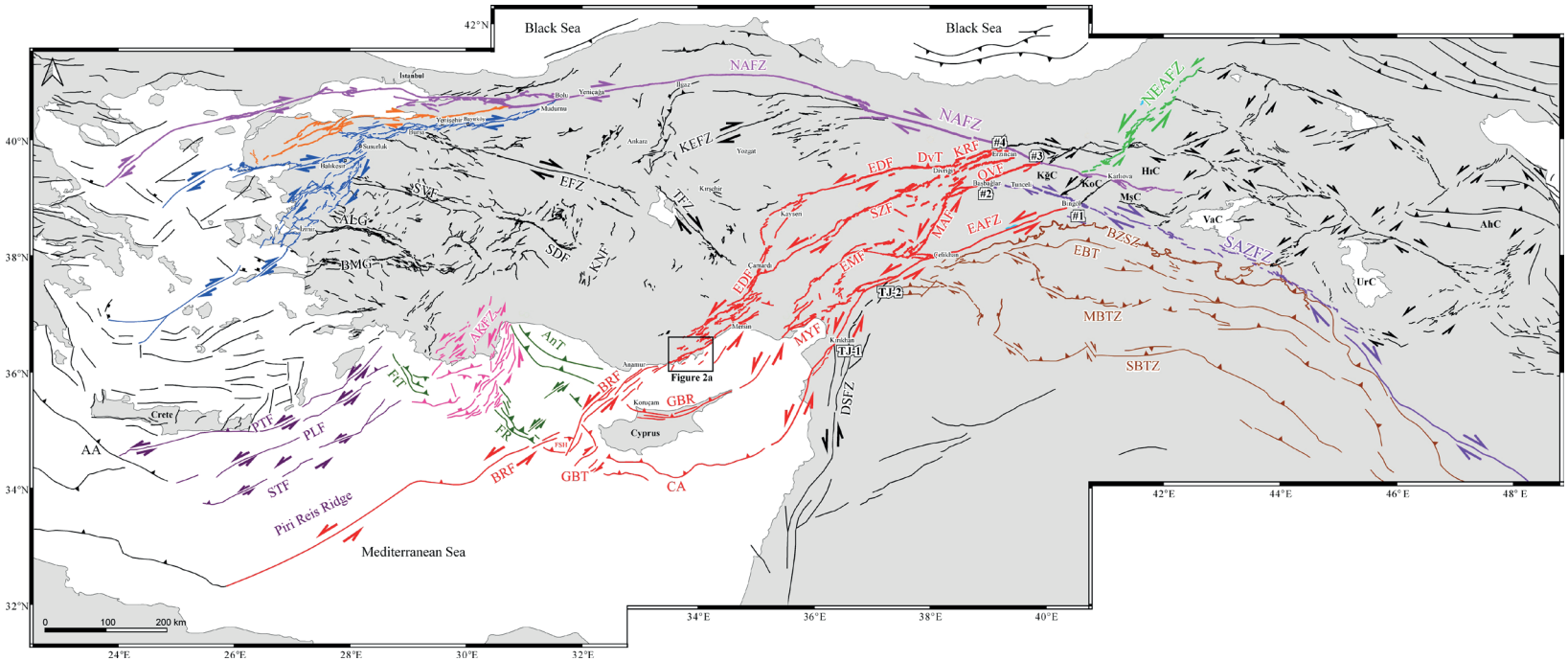

Figure 1. Active fault map of the eastern Mediterranean. Brown lines belong to Southeast Anatolian Wedge structures (Seyitoğlu et al. 2017). BZSZ: Bitlis-Zagros Suture Zone; EBT: Ergani-Silvan Blind Thrust; MBTZ: Mardin Blind Thrust Zone; SBTZ: Sincar-Kerkük Blind Thrust Zone; DSFZ: Dead Sea Fault Zone. Black lines in the Turkish Iranian Plateau represent mainly rhomboidal cell margins (Seyitoğlu et al. 2018). Rhomboidal cells: KğC: Kığı, KoC: Karlıova, MşC: Muş, HıC: Hınıs, VaC: Van, UrC: Urmiye, and AhC: Ahar. For regionwide shear zones, purple lines represent SAZFZ: Southeast Anatolian Zagros Fault Zone; green lines indicate NEAFZ: Northeast Anatolian Fault Zone, fuchsia lines show main branch of NAFZ: North Anatolian Fault Zone. Orange lines indicate middle branch of North Anatolian Fault. Blue lines are the southern branch of North Anatolian Fault Zone (Seyitoğlu et al. 2022c). Red lines show the Anatolian Diagonal Shear Zone (Seyitoğlu et al. 2022a and this paper). EAFZ: East Anatolian Fault Zone; KRF: Karaca Fault; EDF: Ecemiş-Deliler Fault; DvT: Divriği Thrust; OVF: Ovacık Fault; SZF: Sarız Fault; MAF: Malatya Fault; EMF: Elbistan-Misis Fault; MYF: Maraş-Yumurtalık Fault; BRF: Biruni Fault; FSH: Fuat Sezgin High; GBT: Gazi Baf Transform; GBR: Girne-Beşparmak Range; CA: Cyprus Arc. Fault lines on Northern Cyprus are from Elmacı et al. (2025). All other fault lines are modified after Barrier et al. (2004), Emre et al. (2013), and Seyitoğlu et al. (2017; 2018; 2022a, b). KEFZ: Kırıkkale-Erbaa Fault Zone; TFZ: Tuzgölü Fault Zone; EFZ: Eskişehir Fault Zone; SDF: Sultandağı Fault; KNF: Konya Fault; SVF: Simav Fault; SDF: Sultandağı Fault; KNF: Konya Fault; ALG; Alaşehir Graben; BMG: Büyük Menderes Graben; AnT: Antalya Thrust; FR: Florence Rise; AKFZ: Antalya-Kekova Fault Zone; FtT: Fethiye Thrust; PTF: Ptolemy Fault; PLF: Pliny Fault; STF: Strabo Fault. AA: Aegean Arc.

Şekil 1. *Doğu Akdeniz'e ait aktif fay haritası. Kahverengi çizgiler Güneydoğu Anadolu Kama yapılarına aittir (Seyitoğlu vd. 2017). BZSZ: Bitlis-Zagros Kenet Zonu; EBT: Ergani-Silvan Kör Bindirmesi; MBTZ: Mardin Kör Bindirme Zonu; SBTZ: Sincar-Kerkük Kör Bindirme Zonu; DSFZ: Ölüdeniz*

Fay Zonu. Türk-İran Platosu'ndaki siyah çizgiler ağırlıklı olarak romboidal hücre kenarlarını temsil eder (Seyitoğlu vd. 2018). KğC: Kığı, KoC: Karlıova, MşC: Muş, HıC: Hınıs, VaC: Van, UrC: Urmiye, AhC: Ahar romboidal hücreleri. Bölge genelindeki makaslama zonları, mor çizgiler SAZFZ'yi temsil eder: Güneydoğu Anadolu Zagros Fay Zonu; Yeşil çizgiler NEAFZ Kuzeydoğu Anadolu Fay Zonu, fuşya renkli çizgiler ise NAFZ Kuzey Anadolu Fay Zonu, ana kolunu göstermektedir. Turuncu çizgiler Kuzey Anadolu Fay Zonu'nun orta kolunu göstermektedir. Mavi çizgiler Kuzey Anadolu Fay Zonu'nun güney kolunu göstermektedir (Seyitoğlu vd. 2022c). Kırmızı çizgiler Anadolu Çaprazı Makaslama Zonu'nu göstermektedir (Seyitoğlu vd. 2022a ve bu makale). EAFZ: Doğu Anadolu Fay Zonu; KRF: Karaca Fayı; EDF: Ecemiş-Deliler Fayı; DvT: Divriği Bindirmesi; OVF: Ovacık Fayı; SZF: Sarız Fayı; MAF: Malatya Fayı; EMF: Elbistan-Misis Fayı; MYF: Maraş-Yumurtalık Fayı; BRF: Biruni Fayı; FSH: Fuat Sezgin Yükselimi; GBT: Gazibaf Transform Fayı; GBR: Girne-Beşparmak Sıradağları; CA: Kıbrıs Yayı. Kuzey Kıbrıs'taki fay hatları Elmacı vd. (2025)'den alınmıştır. Diğer tüm fay hatları Barrier vd. (2004), Emre vd. (2013), Seyitoğlu vd. (2017; 2018; 2022a, b)'den sonra değiştirilmiştir. KEFZ: Kırıkkale-Erbaa Fay Zonu; TFZ: Tuzgölü Fay Zonu; EFZ: Eskişehir Fay Zonu; SDF: Sultandağı Fayı; KNF: Konya Fayı; SVF: Simav Fayı; KNF: Konya Fayı; ALG; Alaşehir Grabeni; BMG: Büyük Menderes Grabeni; AnT: Antalya Bindirmesi; FR: Florence Yükselimi; AKFZ: Antalya-Kekova Fay Zonu; FtT: Fethiye Bindirmesi; PTF: Ptolemy Fayı; PLF: Pliny Fayı; STF: Strabo Fayı. AA: Ege Yayı

In this paper, we examine morphotectonic features from the southwest end of the Ecemiş-Deliler Fault onshore and provide segment distribution for the Biruni Fault by using offshore seismic reflection sections from Turkish Petroleum (TPAO). In addition, focal mechanism solutions for seismic events attributed to Biruni Fault will be presented. A detailed description of the Biruni Fault will clarify the connection of the northwest margin of the active Anatolian Diagonal to the Cyprus Arc and we will discuss its implications for the neotectonic framework of the Eastern Mediterranean.

MORPHOTECTONICS OF THE SOUTHWESTERN END OF THE ECEMİŞ-DELİLER FAULT

The earliest studies recognised the position of the EDF in the Anatolian Diagonal (Seyitoğlu et al., 2022a). It was named as the Ecemiş Corridor (Blumental, 1941; 1952), the Tekir Dislocation (Metz, 1956), the Ecemiş Fault (Ketin, 1960), the Ecemiş Transcurrent Fault (Pavoni, 1961), the Pozantı- Kayseri Fault (Scott, 1981) and the Ecemiş Fault Zone (Yetiş, 1978; Dirik and Göncüoğlu, 1996).

The Ecemiş Fault and the Deliler Fault were defined as two separate faults to the south and northeast of Kayseri (Emre et al., 2013). The term Central Anatolian Fault Zone was introduced by Koçyiğit and Beyhan (1998), without clear relationship to the NAFZ and the Cyprus Arc. Darin and Umhoefer (2019) clearly defined the northeast end of the EDF while Akyüz et al. (2012) provided palaeoseismological data from trenches near Alaca. A detailed examination of the structural features in the original location of the Ecemiş Fault was presented by Jaffey and Robertson (2001). Around Kayseri, the morphotectonic, kinematic and geochronological evidence for Quaternary activity on the EDF were presented by Higgins et al. (2015), Sarıkaya et al. (2015a, b) and Yıldırım et al. (2016), while the paleomagnetic characteristics of the EDF were also studied (Tatar et al., 2000).

The southwestern end of the EDF is studied relatively less well. İnan and Ekingen (2007) presented structural and morphological evidence for the Namrun Fault. The geological map of southwestern Silifke indicates several semi-parallel, northeast-southwest trending faults (Alan et al., 2014). Although some of them limit Quaternary slope deposits, none of them were described as an active fault.

The block model for the region indicates that the left-lateral slip rate along the southwestern

sector of the EDF ranges from 7.5±1.1 mm/yr in the northeast to 2.8±1.5 at its southwestern end. In its offshore continuation, the slip rate increases south-westward from 4.2 ± 1.8 to 11.7 ± 0.9 mm/yr (Seyitoğlu et al., 2022b). The geomorphic expression of the southwestern EDF is more distinct as a linear trend compared to the northeastern sector. In the southwestern sector, the fault is a wide shear zone up to 20 km, consisting of northeast-southwest trending en-echelon left-lateral faults running parallel to the coastline (Figure 2). At the southwestern end, the shear zone consists of 1.5 km, 2 km and 7 km long segments (EDF-1a to EDF-1c) arranged in a left-stepping pattern. These faults are expressed as linear valleys oriented with northeast-southwest direction. Along EDF-1c, a shear zone in the Palaeozoic bedrock was associated with the EDF together with left-lateral displacement of 1240 m and 60 m along a Quaternary stream (Seyitoğlu et al., 2022a) (Figure 2). Further to the northeast, EDF-1c exhibits a left-lateral arrangement with EDF-1d and its northeastern continuation, EDF-1e. In the northern block of EDF-1e, the northeast-southwest trending Hırmanlı Dere valley is observed, which hosts the village of Hırmanlı (Figure 2). To the south, a distinct Quaternary alluvial fan deposit extends in front of this valley, while the stream bends 1 km to the southwest along the fault, reaching the step-over associated with EDF-1d. In addition, a well-defined saddle is present along EDF-1e near the fan apex. Moreover, a left-lateral offset of 543 m was observed in a river in the northeast sector of the alluvial fan (Seyitoğlu et al., 2022a) (Figure 2).

Further to the northeast, the 5 km-long EDF-2 segment has a right-lateral arrangement with EDF-1e. These segments form the northwestern margin of a northeast-southwest trending trough, filled with Quaternary deposits, and defines the northwestern part of the shear zone. The southeastern margin of the trough is bounded by EDF-5a and EDF-6. The southwest-dipping depression is drained by a river that flows close to EDF-5a. An elongate ridge was observed between EDF-5a and EDF-6 and is interpreted as a shutter ridge together with the 640 m left-lateral shift along a river (Seyitoğlu et al., 2022a) (Figure 2). The northeastern continuation of EDF-5a is also defined by a trough, which is marked by EDF-5b segment. This linear depression is drained by the Akdere stream, which has a north northwest-south southeast trend upstream and at a bend along the fault, flows towards the northeast for about 3 km (Seyitoğlu et al., 2022a). The southeastern margin of the shear zone is further defined by the 1 km-long EDF-5c and the 4.5 km-long EDF-5d. In the northwestern sector, the shear zone, defined by EDF-1e and EDF-2 to the southwest, is delineated by EDF-3 and EDF-4 to the northeast. These faults exhibit a right-lateral pattern, and their interaction results in widening of the shear zone. The 10 km-long EDF-3 fault marks the boundary between bedrock and Quaternary talus deposits, and 345 m left-lateral displacement was measured in the upstream section of the Akdere stream (Seyitoğlu et al., 2022a). The 18 km-long EDF-4 segment is characterised by a linear trace in the bedrock, which affects the Quaternary river pattern (Seyitoğlu et al., 2022a) (Figure 2).

Further to the northeast, the shear zone widens up to 16 km and is defined by EDF-4c and EDF-4b in the northwestern sector, EDF-4a in the central part, and EDF-5e in the southeastern sector. These fault segments are significant as they laterally shift the Göksu River, which is one of the longest rivers in the Taurus Mountains with 260 km length (Figure 2). The river has two main tributaries including, (1) the east-west-oriented Ermenek River and (2) the northwest-southeast-oriented Göksu River. These tributaries merge southwest of Mut to form the main course of the Göksu River, which follows a predominantly northwest-southeast orientation except where it deviates along fault-driven bends.

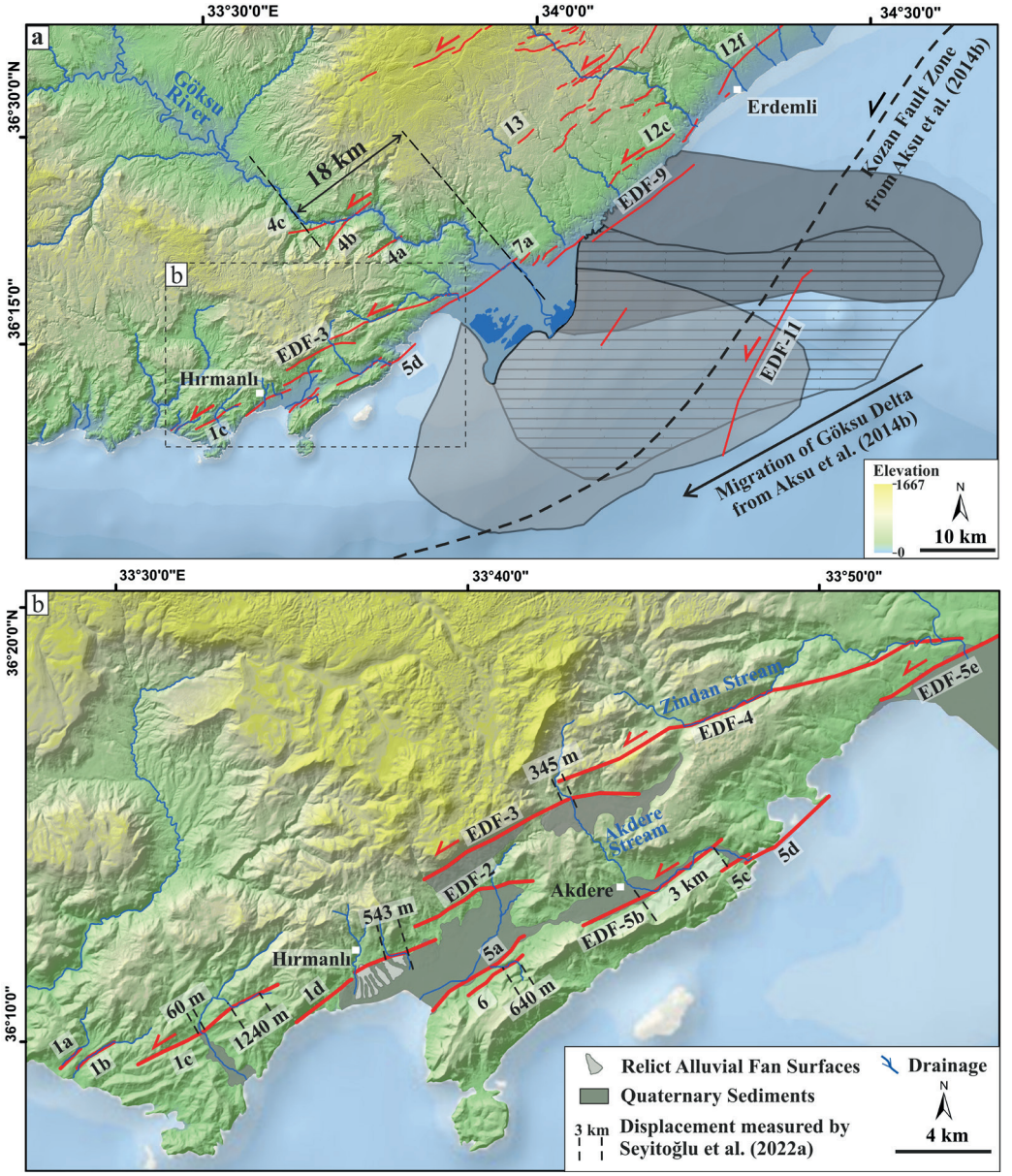

Figure 2. a) The southwestern extension of the Ecemiş–Deliler Fault, showing fault segments adapted from Seyitoğlu et al. (2022a). The 18 km sinistral offset of the Göksu River is measured along the shear zone associated with the EDF. The southward migration of the Göksu Delta lobes and the location of Kozan Fault are shown after Aksu et al. (2014b), indicating that the shifting of the Göksu Delta is better explained by Ecemiş-Deliler fault segments running parallel to the coast rather than the Kozan Fault. **b)** Quaternary geomorphic features around the southwestern termination of the EDF, including the left-lateral offsets measured by Seyitoğlu et al. (2022a).

Şekil 2. a) *Ecemiş–Deliler Fayı'nın güneybatı uzanımı; fay segmentleri Seyitoğlu vd. (2022a)'den uyarlanmıştır. Göksu Nehri'nin 18 km'lik sol yanal ötelenmesi, EDF ile ilişkili makaslama zonu boyunca ölçülmüştür. Göksu Deltası loblarının güneye doğru göçü ve Kozan Fayının konumu Aksu vd. (2014b)'ten uyarlanmıştır. Göksu delta loblarının yer değiştirmesi Kozan Fayından ziyade kıyıya paralel uzanan Ecemiş-Deliler fay segmentleri tarafından daha iyi açıklanmaktadır.* ***b)*** *EDF'nin güneybatı ucundaki Kuvaterner döneme ait jeomorfolojik yapılar; Seyitoğlu vd. (2022a) tarafından ölçülen sol yanal ötelenmeleri içermektedir.*

Along its course, the river has incised into Palaeozoic and Mesozoic basement units, which are unconformably overlain by Miocene marls and carbonates deposited in marine environments (Alan et al., 2014). The youngest marine sediments overlying the surface in the upper course of the river are dated to ca. 8 Ma (Cosentino et al., 2012). The uplift of the region has resulted in a highly incised antecedent valley, especially downstream of the river (Cosentino et al., 2012; Schildgen et al., 2012; Kuzucuoğlu et al., 2019). Left-lateral displacements along the river were measured along the EDF segments by Seyitoğlu et al. (2022a; Appendix A). Specifically, displacements of 385 m were reported along EDF-4a, 1450 m along EDF-4b and 1760 m along EDF-5e. While these measurements indicate displacement along these segments, a comprehensive assessment of lateral shift along the entire shear zone is necessary for more accurate measurement along the river course (e.g., Şengör, 2017). According to this, 18 km lateral displacement is measured between the northwest-southeast oriented river path across the shear-zone. To calculate the long-term slip rate, the age of the youngest marine deposits in the upper course of the river has been used. This provides a regional upper limit for surface emergence, and was adopted here as the maximum possible age constraint since the actual establishment of the drainage system must have postdated the transition to terrestrial conditions. According to this assumption, a minimum long-term slip rate of 2.25 mm/yr has been calculated for the EDF shear zone.

At the mouth of the Göksu River, the Göksu Delta formed, which is bounded by EDF-5e and its northeastern continuation EDF-8. Between these segments, the EDF-7 a-c segments were also identified with left-stepping arrangement on the bedrock. Slickenlines observed along EDF-5e on Mesozoic limestone indicate strike-slip motion (Seyitoğlu et al., 2022a; Appendix A). Similarly, in a cataclastic zone in the Miocene limestone unit, slickenlines and a flower structure provide evidence of deformation along EDF-7a (Seyitoğlu et al., 2022a; Appendix A). According to Aksu et al. (2014a, b), the delta lobes of the Göksu River migrated towards the southwest (Figure 2a). This deformation was identified from seismic reflection profiles and is dated to Pliocene-Quaternary based on stratigraphic units corelated with well data and tentatively linked to exposed units on land. In their interpretation, the lateral migration of the delta exceeds 20 km, and this migration is associated with the Kozan Fault zone. However, this fault is located parallel to the coast at a considerable distance, and its proposed position must have caused truncation at the southwestern edge of the delta, interpreted as being offset (Figure 2a). In contrast, the results of the present study suggest an alternative explanation: the migration of the delta lobe can be temporally and spatially correlated with the lateral shift of the Göksu River, which is associated with activity on the EDF. Based on the delta lobe migration inferred by Aksu et al. (2014a, b), the implied slip rate for the EDF would be ~3.8 mm/yr during the Pliocene-Quaternary time interval. The contrast with the minimum long-term slip rate of 2.25 mm/yr (since 8 Ma) indicates that slip along the fault was likely non-uniform, with alternating phases of acceleration and deceleration over geological timescales. The pronounced Quaternary morphology observed along the EDF in this study is likely associated with this higher slip rate.

THE BIRUNI FAULT

The offshore continuation of the EDF was previously only estimated based on bathymetry between Anatolia and west of Cyprus and shown with a question mark (Koçyiğit and Beyhan, 1998). More comprehensive offshore data were provided by Aksu et al. (2005; 2014a, b).

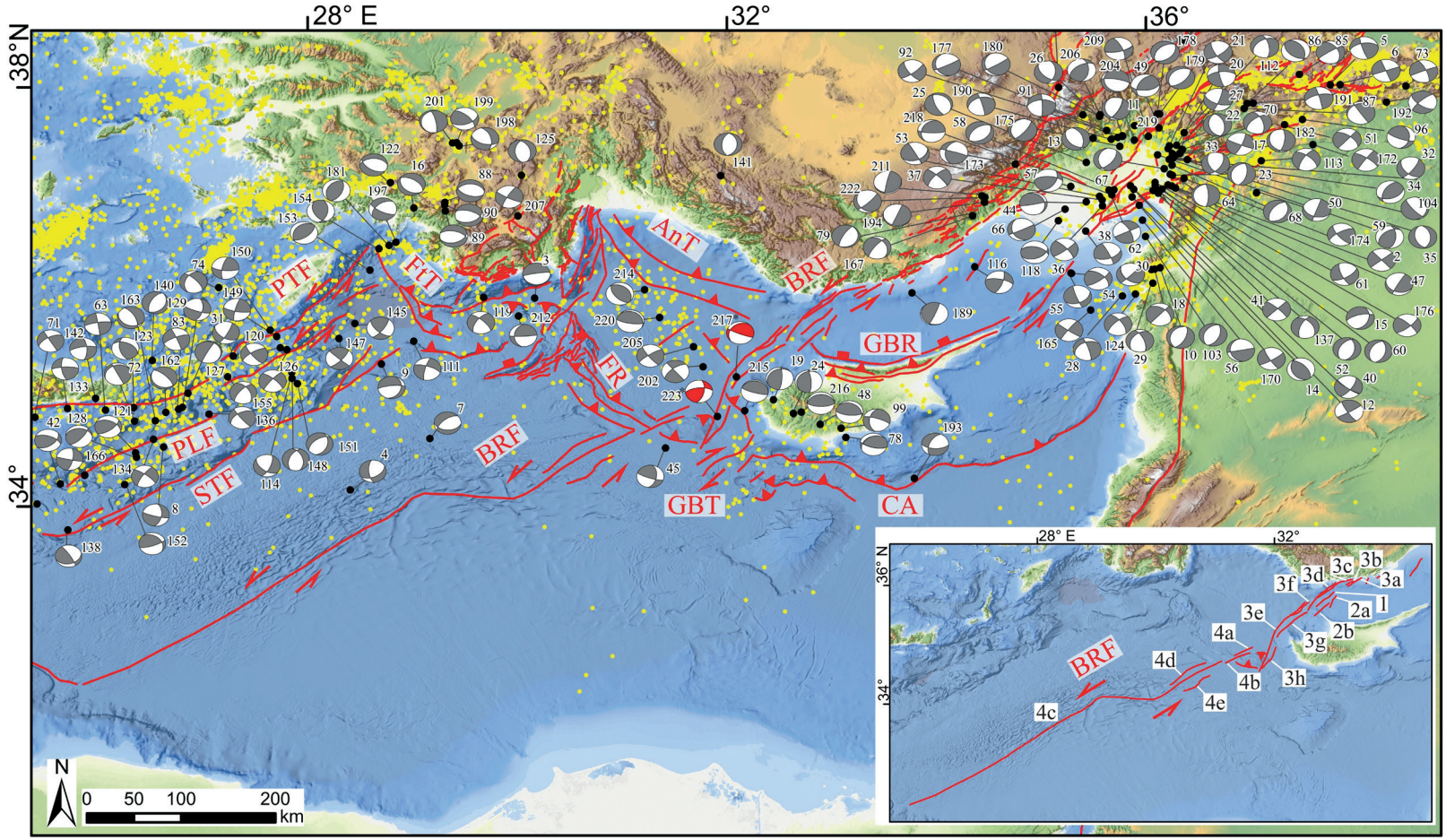

Figure 3. Active fault map of the eastern Mediterranean. Seismicity in the region is shown with yellow dots, representing earthquake epicentres with magnitudes ≥3.5 and depths <30 km obtained from the Republic of Turkey Ministry of Disaster and Emergency Management Authority (AFAD). The numbering of the focal mechanism solutions for earthquakes up to event number 214 is adapted from Seyitoğlu et al. (2022a). For events numbered 215 and above, please refer to Table 1 for the new solutions presented in this study. The inset map shows the segment distribution of the Biruni Fault.

Şekil 3. *Doğu Akdeniz'in aktif fay haritası. Bölgedeki sismik aktivite, T.C. İçişleri Bakanlığı Afet ve Acil Durum Yönetimi Başkanlığı (AFAD) verilerine dayalı olarak, büyüklüğü ≥3.5 ve odak derinliği <30 km olan depremlerin dışmerkezlerini temsil eden sarı noktalarla gösterilmiştir. 214 numaralı olaya kadar olan deprem odak mekanizması çözümlerinin numaralandırması Seyitoğlu vd. (2022a) çalışmasından uyarlanmıştır. Bu çalışmada sunulan yeni çözümler için 215 ve üzeri numaralı olaylara ilişkin veriler Çizelge 1'de sunulmuştur. Köşedeki haritada Biruni Fayı'nın segment dağılımı gösterilmektedir.*

The Kozan Fault zone, which runs parallel to the western coast of the Mersin Gulf, is proposed to be an equivalent of the offshore Ecemiş fault complex of Özel et al. (2007). The delta lobe shifting of the Göksu River (Aksu et al., 2014a, b) was attributed to the Kozan Fault zone, although it is located away from the western margin of Mersin Gulf.

The Biruni Fault is identified as an offshore continuation of the left-lateral strike-slip EDF of the Anatolian Diagonal by re-interpreting seismic reflection sections from Mansfield (2005) and Aksu et al. (2005; 2014a, b). However, the data from seismic sections were not published due to the lack of copyright permission (Seyitoğlu et al., 2022a).

In this section, we present our interpreted seismic sections obtained from TPAO and produce a map of the fault segments with precise/reliable coordinate system (Figure 3)

The position of the offshore Biruni Fault can be seen in seismic reflection line CrS-1 where a positive flower structure is observed between segments BRF-3d and BRF-3c at the northwestern end (Figure 4). A prominent morphological trough on the sea floor corresponds to segment BRF-1. Segment BRF-2a also presents as a typical flower structure (Figure 4). The northern margin of the Girne-Beşparmak Range (GBR) is interpreted as a normal fault, following Calon et al. (2005) (Figures 3 & 4).

Further to the southwest, the nearly north-south trending Line 08 crosscuts the BRF-3f, BRF-3e and BRF-3g segments, which create a prominent morphological trough on the sea floor due to their negative flower structure (Figure 5).

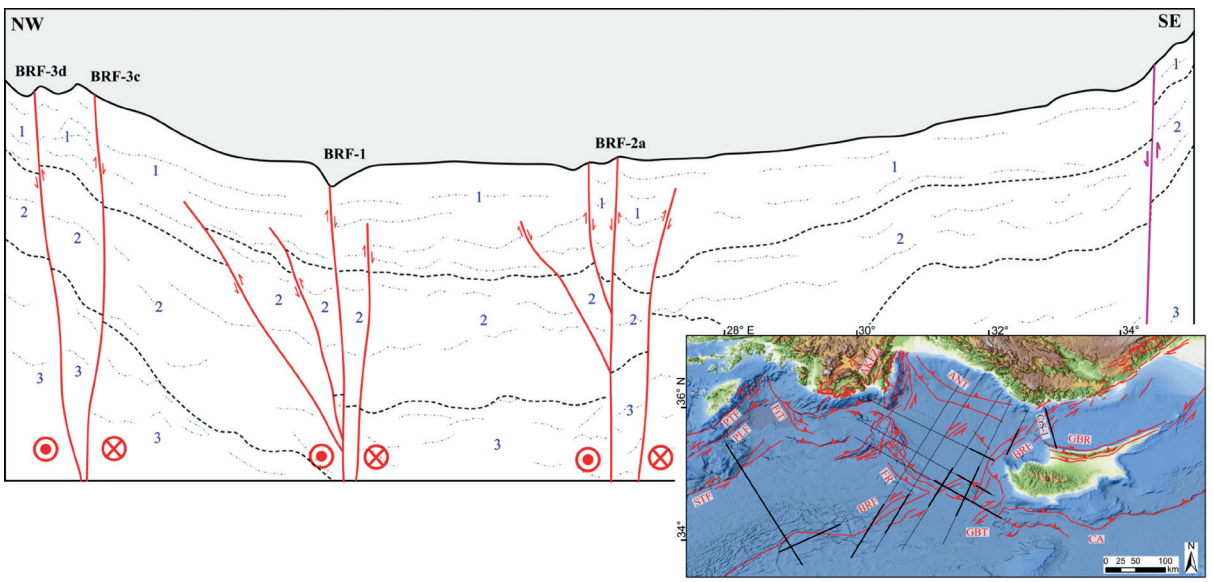

Figure 4. Geological cross section based on seismic reflection profile from Turkish Petroleum (CrS-1). 1: Pliocene-Quaternary clastic deposits, 2: Messinian evaporites, 3: Pre-Messinian deposits.

Şekil 4. *Türkiye Petrolleri'ne ait CrS-1 sismik yansıma profiline dayalı jeolojik kesit. 1: Pliyosen–Kuvaterner kırıntılı tortullar, 2: Messiniyen evaporitleri, 3: Messiniyen öncesi çökeller.*

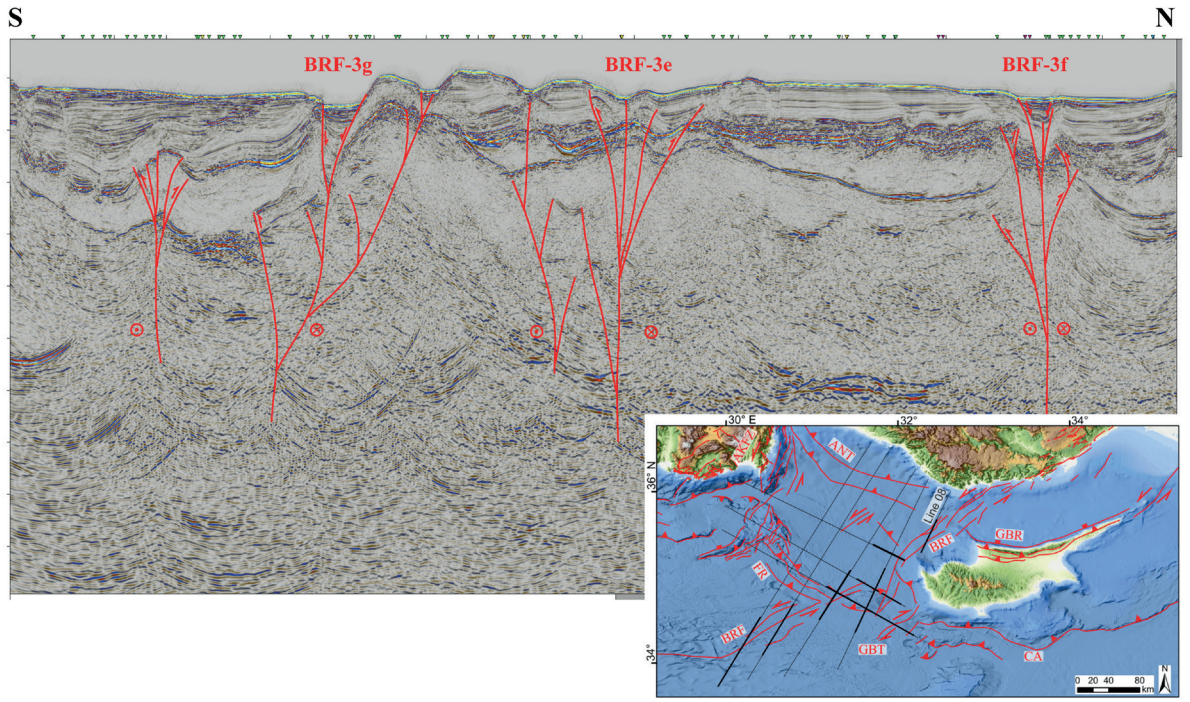

Figure 5. Seismic reflection section Line 08.

Şekil 5. *Hat 08 sismik yansıma kesiti.*

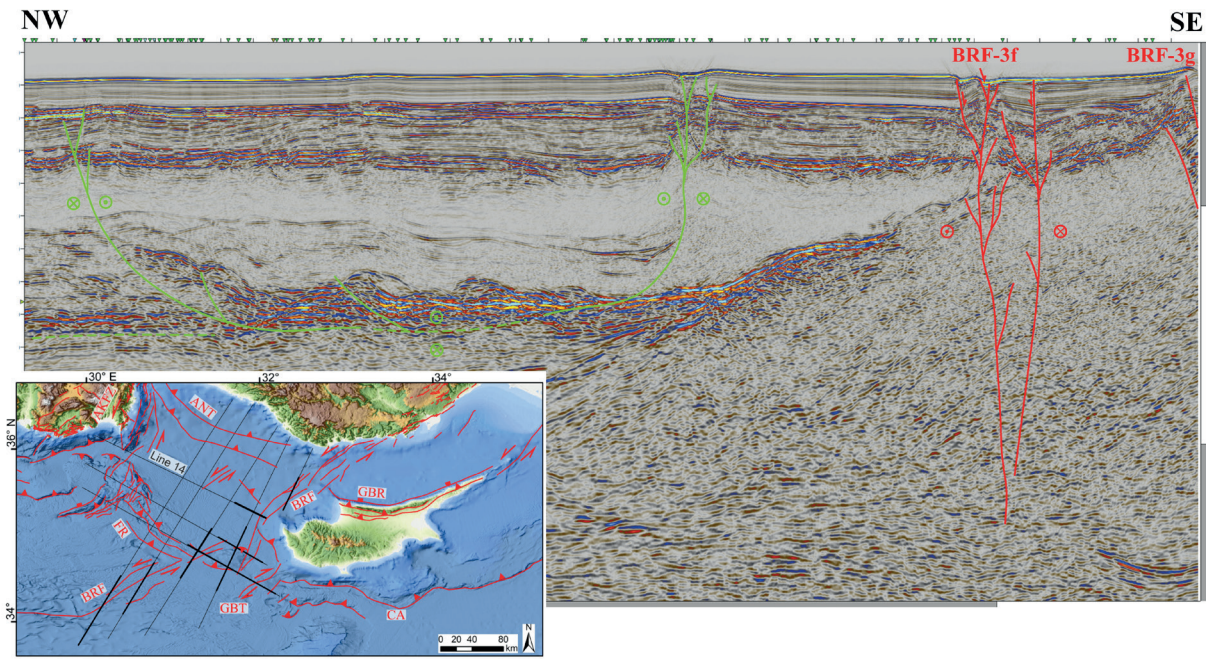

Figure 6. Seismic reflection section Line 14.

Şekil 6. *Hat 14 sismik yansıma kesiti.*

Line 14 shows the southwestern continuation of segment BRF-3f, which is clearly recognised by the deformation of the uppermost seismic layers. Traces of segment BRF-3g are seen at the southeastern margin of the seismic section. The deformations of the seismic layers to the northwest are attributed to the edges of thrust sheets, because they cannot be traced as a deeper structure. These are represented by green lines in Figure 6.

Segment BRF-3f and semi-parallel segment BRF-3h can be distinguished on the southeastern margin of Line 15. On its northwestern margin, segment BRF-4a is easily differentiated after Woodside et al. (2002; Fig. 7) (Figure 7). The semi-parallel BRF-4b and the southernmost tip of BRF-3f are also seen on Line 16 (Figures 7 & 8). Line 15 and Line 16 indicate that the Biruni fault segments create a restraining stepover where a pressure ridge called the Fuat Sezgin High (FSH) developed. The segments of the Biruni Fault limiting the FSH (i.e., BRF-3f and BRF-4a, BRF-4b) show transpressive character, and the thrusts creating the FSH are marked as green lines in Figures 7 and 8. The thrust-related structure of FSH is more clearly observed along the northeast-southwest trending Line 07 (Figure 9). This structure was interpreted differently as the Florence Rise (Güneş et al., 2018; see their Line D).

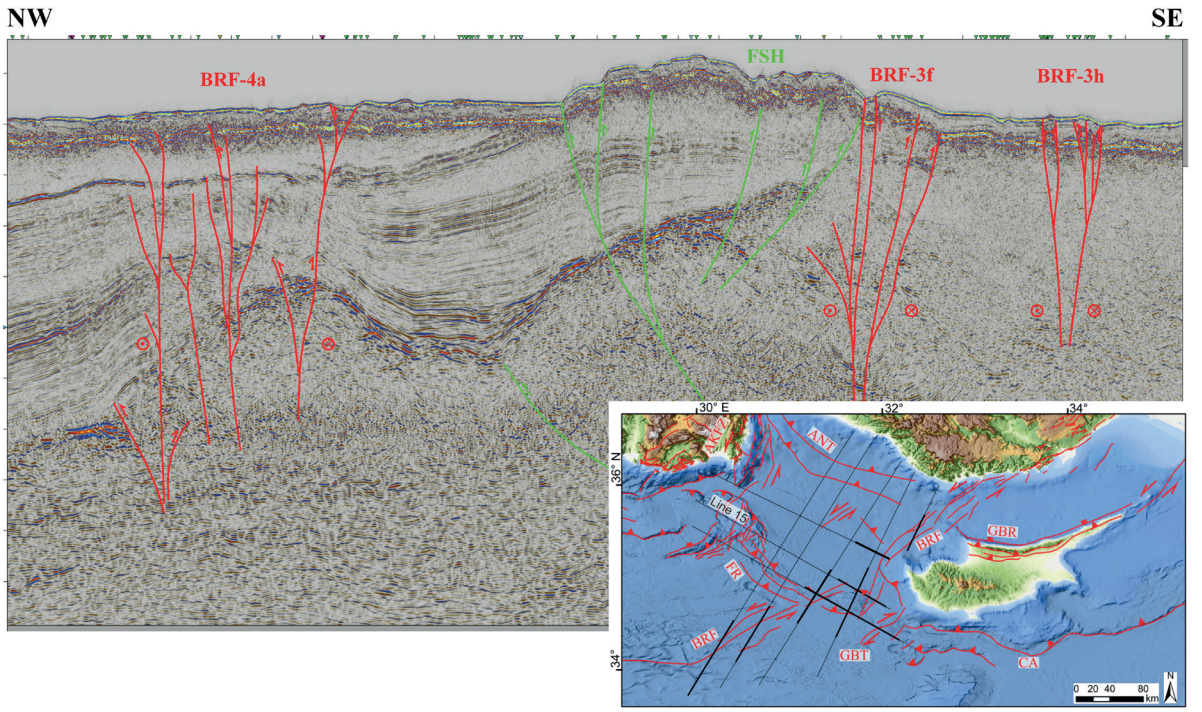

Figure 7. Seismic reflection section Line 15.
Şekil 7. *Hat 15 sismik yansıma kesiti.*

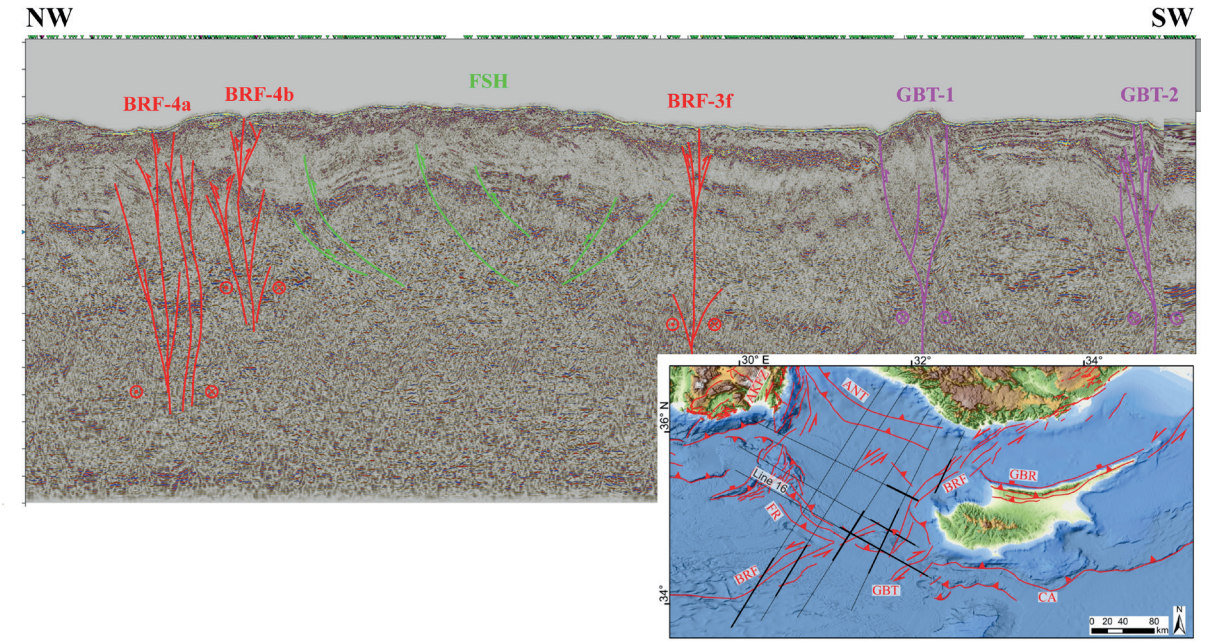

Figure 8. Seismic reflection section Line 16.
Şekil 8. *Hat 16 sismik yansıma kesiti.*

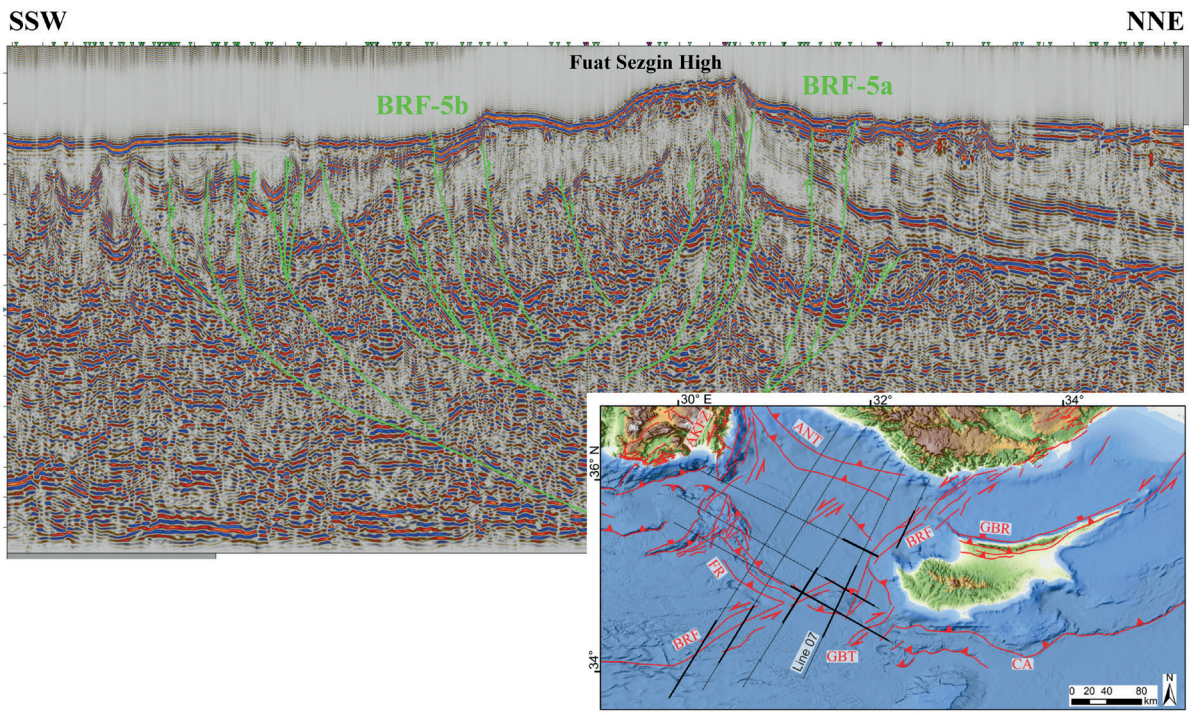

Figure 9. Seismic reflection section Line 07.
Şekil 9. *Hat 07 sismik yansıma kesiti.*

It should be noted that the southwest side of Line 16 also indicates the position of the right-lateral Gazibaf (Paphos) transform faults (GBT-1 and GBT-2) (Seyitoğlu et al., 2022a), which are associated with a prominent morphological high developed between the thrusts of Cyprus Arc. These have produced significant earthquakes with right-lateral focal mechanism solutions (Arvidsson et al., 1998; Pilidou et al., 2004; Symeou et al., 2018) (Figures 3 & 8).

The semi-parallel segments BRF-4a and BRF-4b, limiting the northwest margin of FSH, are seen on the northwest side of Line 16 (Figure 8). The southwest continuation of segment BRF-4b is clearly distinguished on the northeast-southwest trending Line 06 where the green-coloured thrusts located on the northeastern side of BRF-4b represent thrusts between the Florence Rise and the Antalya Thrust. However, the thrusts on the southwestern side represent the thrusts developed in front of the FSH (Figure 10).

The northeast-southwest trending Line 05 and Line 04 indicate the presence of three semi-parallel mainly transpressive segments of the Biruni Fault in which the middle segment BRF-4c can be continuously traced (Figures 11 & 12). The geological cross sections based on seismic profiles from TPAO (Figures 13 & 14) demonstrate that the southwest continuation of BRF-4c can be securely extended to the Aegean Arc with a restraining bend (Figures 1 & 3). The southwest extension of the Biruni Fault corresponds to the shear zone between the Northern and Southern Outer Domains of Huguen et al. (2001, see their Fig. 7). In this case, the Ptolemy-Pliny-Strabo Fault Zone and the Biruni Fault are parallel left-lateral structures and the Piri Reis Ridge (Seyitoğlu et al., 2022a), formerly known as the Mediterranean Ridge, developed between them (Figures 1 & 3).

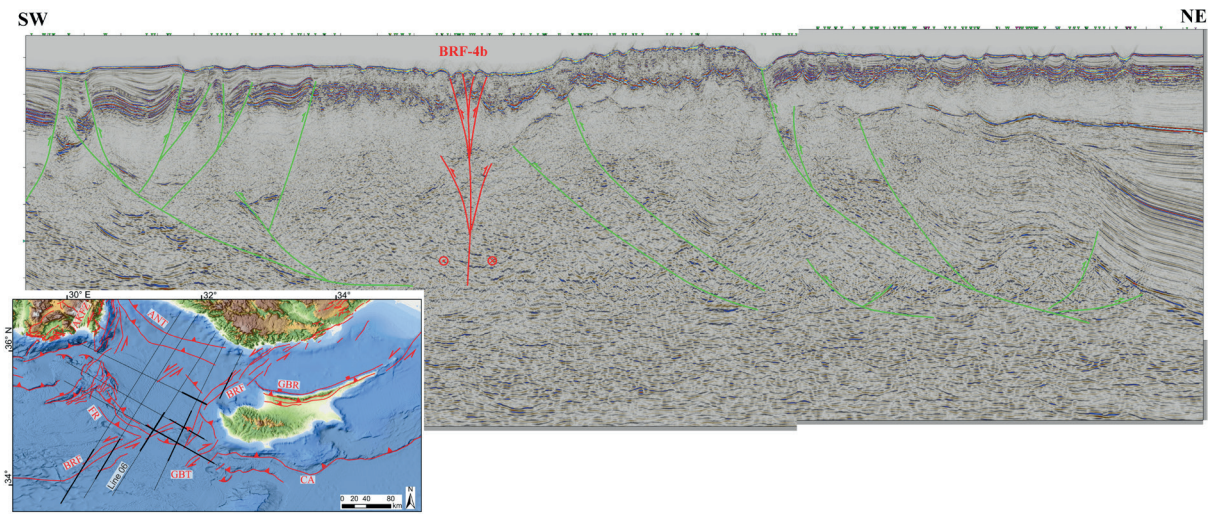

Figure 10. Seismic reflection section Line 06.
Şekil 10. *Hat 06 sismik yansıma kesiti.*

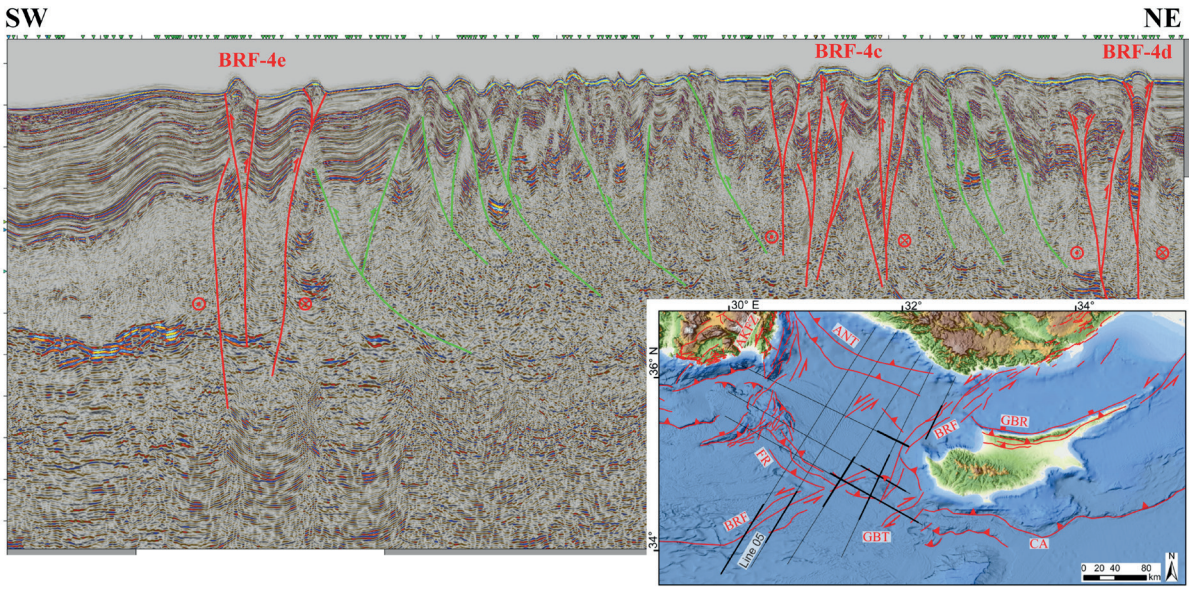

Figure 11. Seismic reflection section Line 05.
Şekil 11. *Hat 05 sismik yansıma kesiti.*

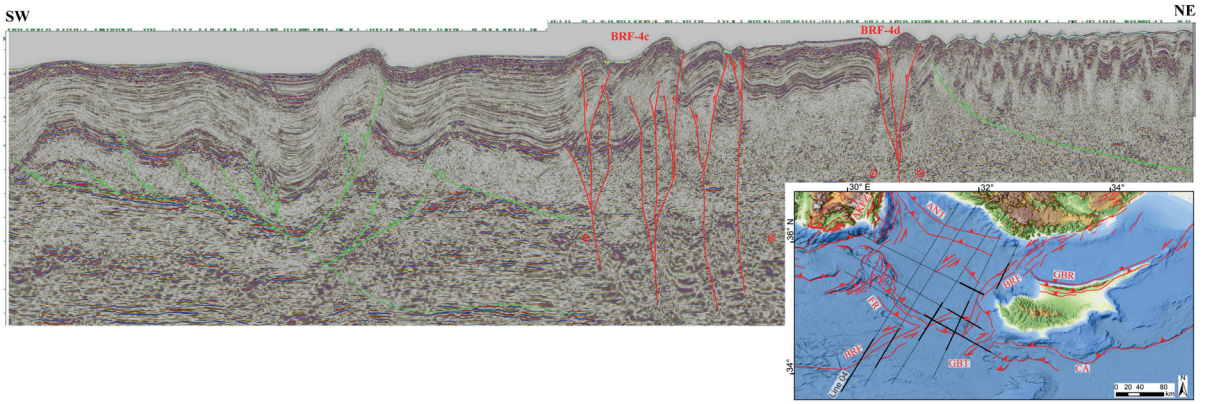

Figure 12. Seismic reflection section Line 04.
Şekil 12. *Hat 04 sismik yansıma kesiti.*

FOCAL MECHANISM SOLUTIONS FOR EARTHQUAKES IN THE STUDY REGION

In this study, the intention was to compute focal mechanism solutions for all earthquakes located within the boundaries of the study area. However, due to difficulties in accessing digital waveform data for older events, the focal mechanisms of earthquakes with magnitudes greater than 4.5 were obtained from established databases such as the Global Centroid Moment Tensor (GCMT) catalogue. For more recent and moderate-magnitude earthquakes (i.e., those with magnitudes below 4.5), efforts were made to compute the solutions directly within the scope of this study. As part of this effort, focal mechanism solutions for two earthquakes were successfully obtained and analysed.

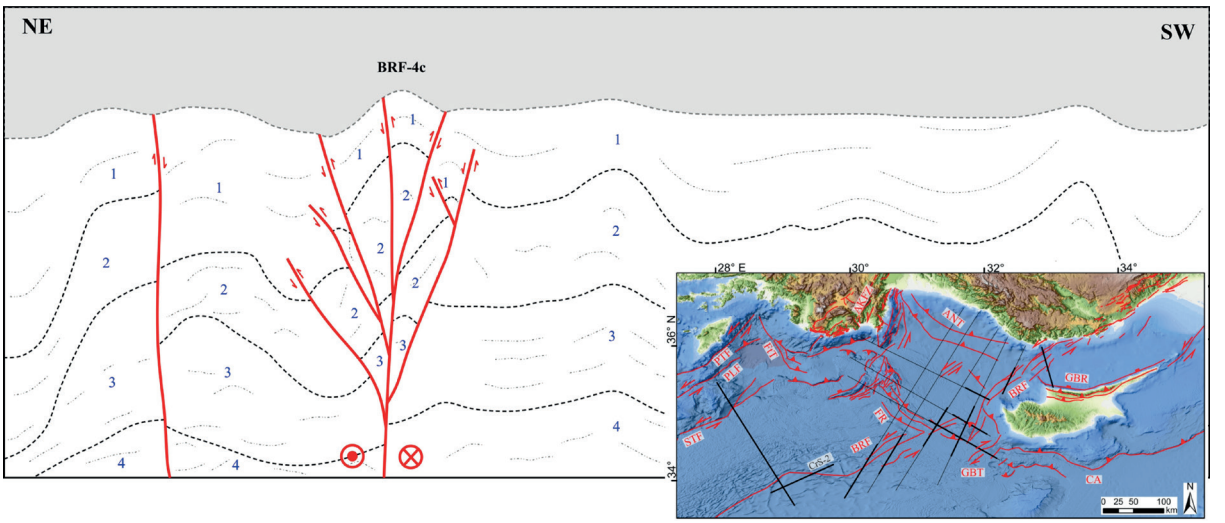

Figure 13. Geological cross section based on seismic reflection profile from Turkish Petroleum (CrS-2). 1: Pliocene-Quaternary clastic deposits, 2: Messinian evaporites, 3: Pre-Messinian deposits, 4: Cretaceous to Eocene deposits.

Şekil 13. *Türkiye Petrolleri'ne ait CrS-2 sismik yansıma profiline dayalı jeolojik kesit.* ***1.*** *Pliyosen–Kuvaterner kırıntılı tortulları,* ***2.*** *Messiniyen evaporitleri,* ***3.*** *Messiniyen öncesi birikintiler,* ***4.*** *Kretase–Eosen çökelleri.*

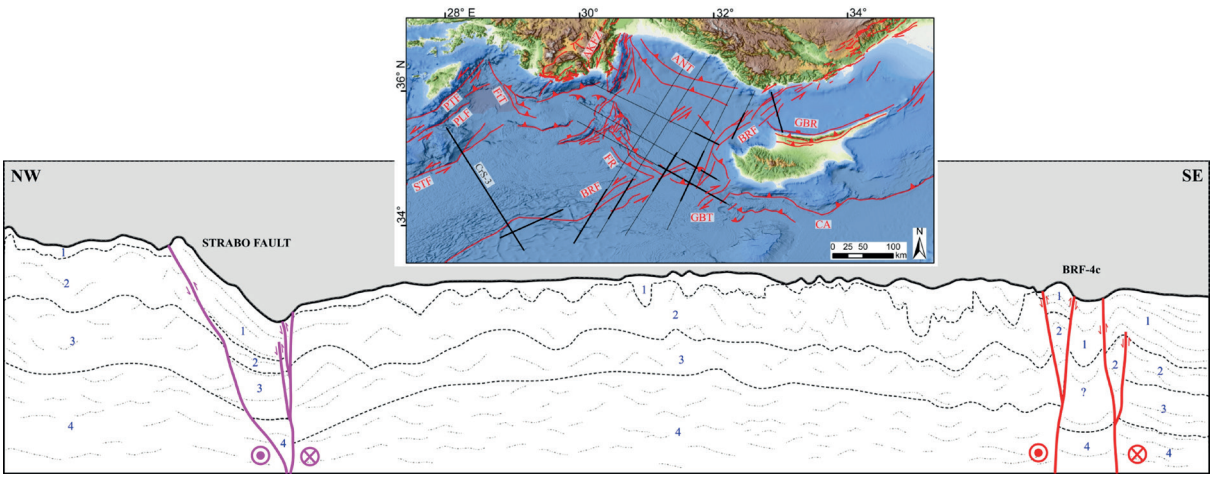

Figure 14. Geological cross section based on seismic reflection profile from Turkish Petroleum (CrS-3). 1: Pliocene-Quaternary clastic deposits, 2: Messinian evaporites, 3: Pre-Messinian deposits, 4: Cretaceous to Eocene deposits.

Şekil 14. *Türkiye Petrolleri'ne ait CrS-3 sismik yansıma profiline dayalı jeolojik kesit.* ***1.*** *Pliyosen–Kuvaterner kırıntılı tortulları,* ***2.*** *Messiniyen evaporitleri,* ***3.*** *Messiniyen öncesi birikintiler,* ***4.*** *Kretase–Eosen çökelleri.*

For the focal mechanism solution analysis, the Regional Moment Tensor (RMT) inversion technique developed by Herrmann (2013) was utilised to determine the focal mechanisms of earthquakes with magnitudes equal to or greater than 3.0. The three-component broadband waveform data necessary for the RMT analysis were acquired from two main sources: the European Integrated Data Archive (EIDA) system (http://www.orfeus-eu.org/data/eida) and Türkiye's Earthquake Data

Centre System (TDVMS) operated by the Disaster and Emergency Management Presidency (AFAD) (https://tdvms.afad.gov.tr/).

Due to the sparse distribution of nearby seismic stations in certain regions, a maximum epicentral distance of 700 km was applied to ensure sufficient data coverage and quality. The waveform data were collected from stations within Türkiye, such as those operated by the Boğaziçi University Kandilli Observatory and Earthquake Research Institute (KOERI) and AFAD, as well as from seismic monitoring centres in neighbouring countries. Most of these stations are equipped with velocity-sensitive broadband seismometers capable of recording high-quality seismic signals.

Since the earthquake locations provided by the data agencies were considered reliable, no additional relocation procedures were undertaken. For the RMT analysis, ground velocity waveforms -both observed and synthetic Green's functions- were extracted within predefined time windows, beginning 5-10 seconds before P-wave arrival and extending up to 110-180 seconds afterward. A three-pole causal Butterworth bandpass filter was applied to the waveforms, typically within the 0.02-0.10 Hz frequency band. However, narrower bands such as 0.06-0.08 Hz or 0.08-0.10 Hz were often preferred to better isolate the seismic signals. In cases with low signal-to-noise ratio, a micro seism rejection filter was optionally employed. During the inversion process, signals with high noise levels or inconsistencies were carefully identified and excluded to maintain the accuracy and reliability of the results.

To demonstrate the application of the RMT method, two recent earthquakes were selected for detailed focal mechanism analysis. The first event occurred on 30.08.2022 at 20:42:31 UTC with local magnitude (Mw) of 4.1 (named Event-1), and the second on 24.12.2024 at 18:22:27 UTC with Mw of 4.0 (named Event-2).

Event-1 and Event-2 were analysed using quality data from 38 and 26 broadband stations, respectively (Figures 15a & 15b). The optimal focal depths were determined through a misfit variance-depth correlation analysis (Figures 16a & 16b), yielding the best fit at a depth of 29 km for Event-1 and of 17 km for Event-2. The comparisons of the observed and synthetic waveforms for selected stations are shown in Figure 17a and Figure 17b, demonstrating a strong correlation and confirming the reliability of the inversion results. The calculated source parameters for both the earthquakes analysed within the scope of this study and those obtained from external seismic data repositories are compiled and presented in Table 1.

The left-lateral nature of the focal mechanism solutions and the location of the 2022 and 2024 events support the view that the Biruni Fault is an active left-lateral structure west of Cyprus.

DISCUSSION

The closure of the Neo-Tethyan ocean between the Arabian Plate and Eurasia since the Late Maastrichtian – Early Eocene along the Bitlis-Zagros Suture Zone (BZSZ) shaped the neotectonic framework of the Eastern Mediterranean (Figure 1). The tectonic escape model was suggested as a consequence of this collision at the beginning of plate tectonics theory and was widely accepted in the following decades (McKenzie, 1972; Hall, 1976; Şengör and Kidd, 1979; Şengör, 1979, 1980; Şengör and Yılmaz, 1981; Aktaş and Robertson, 1984; Şengör et al., 1985; 2019; Yılmaz, 1993). It was postulated that the continental collision created thick crust, resulting in the westward escape of the Anatolian plate along the North Anatolian Fault Zone (NAFZ) and the East Anatolian Fault Zone (EAFZ) (Dewey et al., 1986; Şengör et al., 1985). However, geophysical studies in the following years demonstrated that there is no thick crust in eastern Türkiye and the high topography is explained by asthenosphere-supported thin crust (Şengör et al., 2003; 2008).

It is emphasised that north - south shortening in east and southeast Anatolia is accommodated by the right- and left-lateral strike-slip faults, east-west trending thrusts and fold axes, and north-south trending normal faults. A single interaction point between the right- and left-lateral fault zones around Karlıova was suggested from which the Anatolian plate moves westward (Şengör et al., 1985). GPS studies (i.e. Reilinger et al., 2006) indicate that the slip rate of the right-lateral NAFZ (24 mm/yr) and the left-lateral EAFZ (10-9 mm/yr) are different and do not support a symmetrical escape wedge. Şengör et al. (2019) revised the model as an asymmetrical wedge in Karlıova that requires transpressional movement on the EAFZ (Şengör et al., 2019; Fig. 31). However, as indicated by the focal mechanism solutions of the earthquakes, a transtensional shear exists in the east of the Çukurova area (Seyitoğlu et al., 2022a; Fig. A24 in Appendix A), which may be used against the idea of a single interaction point related to the asymmetrical escape wedge of Şengör et al. (2019).

The deformation resulting from continental collisions in eastern and southeastern Anatolia was recently explained by two different models. In the foreland of BZSZ, the Southeast Anatolian Wedge (SEAW) is defined between BZSZ to the north and Sincar Mountain to the south (Figure 1). Several thrusts/blind thrusts identified by using asymmetrical anticlines in their hanging wall merge into a basal thrust and the thrust sheets are separated by tear faults in the cross sectional and map view of the SEAW, respectively (brown lines in Figure 1). One of the major earthquakes, the 1975.09.06 (M 6.7) Lice earthquake, is attributed to the Ergani-Silvan Blind Thrust (Seyitoğlu et al., 2017).

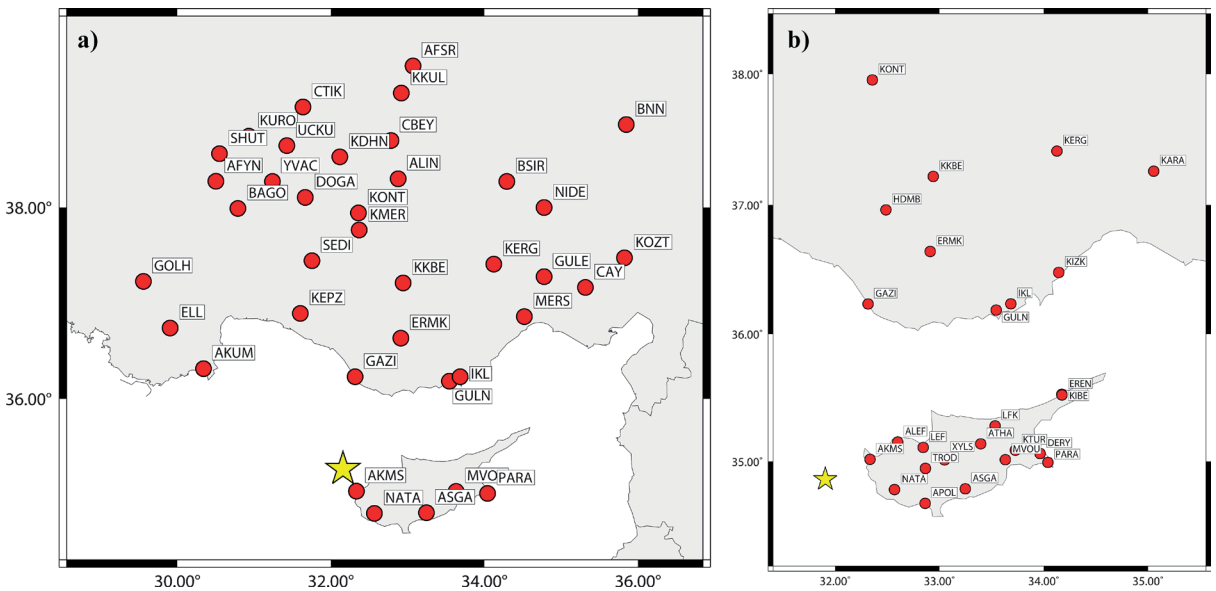

Figure 15. Broadband station distribution (solid circles) used for moment tensor inversion analysis of **(a)** the 30.08.2022 earthquake (UTC 20:42:231; Mw= 4.1) and **(b)** the 24.12.2024 earthquake (UTC 18:22:27; Mw= 4.0). Event locations are indicated with a star.

Şekil 15. *Moment tensör ters çözüm analizinde kullanılan geniş bant istasyon dağılımı (dolu daireler)* ***(a)*** *30.08.2022 tarihli deprem (UTC 20:42:23; Mw = 4.1) ve* ***(b)*** *24.12.2024 tarihli deprem (UTC 18:22:27; Mw = 4.0). Deprem konumları yıldız sembolü ile gösterilmiştir.*

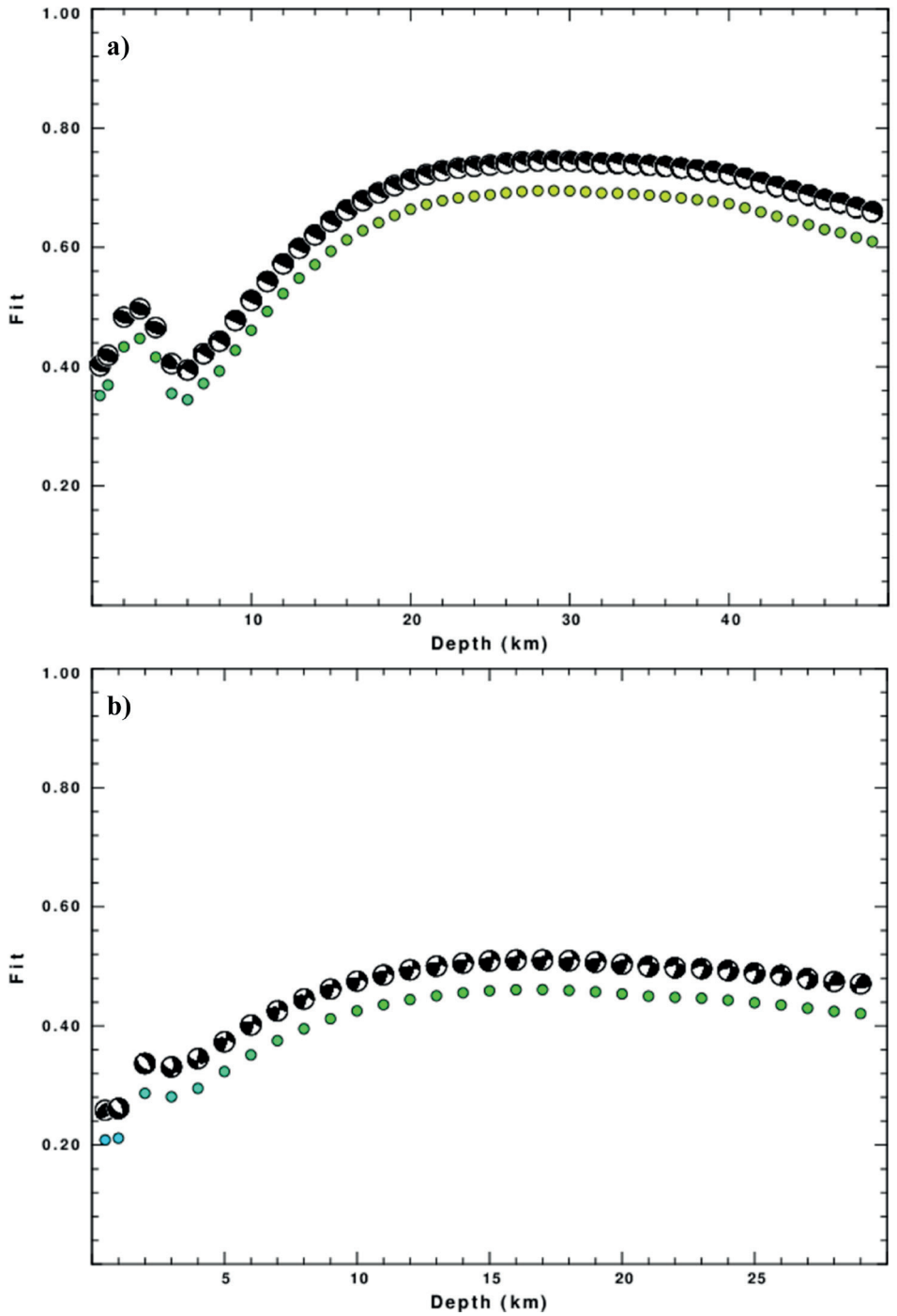

Figure 16. Correlation plot of the reduction in distance-weighted variance against source depth for **(a)** the 30.08.2022 earthquake (UTC 20:42:231; Mw= 4.1) and **(b)** the 24.12.2024 earthquake (UTC 18:22:27; Mw= 4.0). The best fit is provided for a depth of 29 km for Event-1 and 17 km for Event-2.

Şekil 16. (a) *30.08.2022 tarihli deprem (UTC 20:42:23; Mw = 4.1) ve* ***(b)*** *24.12.2024 tarihli deprem (UTC 18:22:27; Mw = 4.0) için kaynak derinliği ile uzaklık arasındaki ağırlıklandırılmış değişinti (varyans) azalım ilişkisi. En iyi uyum, birinci olay için 29 km, ikinci olay için ise 17 km derinlikte sağlanmıştır.*

Figure 17. Observed (red/light grey) and synthetic (blue/dark grey) waveforms for **(a)** the 30.08.2022 earthquake (UTC 20:42:231; Mw= 4.1) and **(b)** the 24.12.2024 earthquake (UTC 18:22:27; Mw= 4.0) are superimposed. Each waveform pair is displayed using the same amplitude scale, with peak values noted to the left of each trace. Time shifts and variance reduction percentages are presented on the right side of each trace, with the time shift as the upper value and variance reduction as the lower. Station codes are listed adjacent to their corresponding waveforms.

Şekil 17. a) *30.08.2022 tarihli deprem (UTC 20:42:23; Mw = 4.1) ve* ***(b)*** *24.12.2024 tarihli deprem (UTC 18:22:27; Mw = 4.0) için gözlemsel (kırmızı/açık gri) ve sentetik (mavi/koyu gri) dalga biçimleri üst üste gösterilmiştir. Her dalga çifti aynı genlik ölçeği kullanılarak sunulmuş olup, tepe değerleri her sinyal izinin sol tarafında belirtilmiştir. Zaman kaymaları ve değişinti (varyans) azaltma yüzdeleri, her izin sağ tarafında gösterilmiştir; üstte zaman kayması, altta ise değişinti azalım değeri yer almaktadır. İstasyon kodları ilgili dalga biçimlerinin yanında listelenmiştir.*

Table 1. Earthquake Focal Parameters and Focal Mechanism Solutions for Major Seismic Events.

Çizelge 1. *Belirli Depremlere Ait Odak Parametreleri ve Odak Mekanizması Çözümleri.*

Earthquake Focal Parameters									Fault Plane Solutions											
#	Date (y.m.d)	Time (GMT) (h:m:s)	Lat. (°N)	Lon. (°E)	Depth (km)	Mag.	M Type	Ref.	Str1 (°)	Dip1 (°)	Rake1 (°)	Str2 (°)	Dip2 (°)	Rake2 (°)	Pazm (°)	Pplg (°)	Tazm (°)	Tplg (°)	Ref.	Beach ball
215	2022.01.11	01:07:46	34,919	32,1663	5.06	6,4	Mw	AFAD	287	11	86	111	79	91	200	34	22	56	USGS	
216	2022.04.26	19:11:37	34,902	32,7058	7,7	4,6	Mw	AFAD	94	66	92	267	23	83	182	21	8	69	KOERI	
217*	2022.08.30	20:42:31	35,2391	32,0866	5,4	4,1	Mw	AFAD	117	82	114	225	25	20	187	33	52	48	This study	
218	2023.03.11	19:35:16	36,976	35,668	7	4	Mw	AFAD	208	31	27	94	77	118	163	26	36	50	AFAD	
219	2023.07.25	05:44:49	37,634	35,884	10,38	5,5	Mw	AFAD	161	76	177	251	88	14	26	8	117	12	KOERI	
220	2023.08.10	13:16:04	35,804	31.351	12,44	4,5	Mw	AFAD	104	74	82	311	16	115	200	29	3	60	KOERI	
221	2023.08.22	10:17:34	38,435	36,675	7,06	4,7	Mw	AFAD	295	90	128	25	38	0	353	34	237	34	USGS	
222	2024.06.26	20:37:12	36,9511	34,4569	16	4,1	Mw	AFAD	47	80	-61	154	31	-160	347	47	114	29	AFAD	
223*	2024.12.24	18:22:27	34,8603	31,9050	9,81	4,3	Mw	AFAD	269	64	146	15	60	30	323	3	42	56	This study	

Note: The numbering of the earthquakes in this table starts from 215, following the last event (No. 214) listed in the earthquake catalogue of Seyitoğlu et al. (2022a). For the focal mechanism solutions shown in Fig. 3, events numbered 1–214 refer to Seyitoğlu et al. (2022a), while events numbered 215 and onward correspond to the data presented in this study.

Abbreviations: Lat.: Latitude**; Lon.:** Longitude**; Mag:** Magnitude**; Str.:** Strike; **Dip:** Dip; **Rake:** Rake; **Pazm:** Pressure azimuth; **Pplg:** Pressure plunge; **Tazm:** Tension azimuth; **Tplg:** Tension plunge; **Mw:** moment magnitude; **USGS:** U.S. Geological Survey. USGS. USA https://earthquake.usgs.gov/earthquakes/search/; **KOERI:** Boğaziçi University Kandilli Observatory and Earthquake Research Institute Regional Earthquake-Tsunami Monitoring Center. http://www.koeri.boun.edu.tr/sismo/

zeqdb/; **AFAD;** Republic of Turkey Ministry of Disaster and Emergency Management Authority. http://www.deprem.gov.tr/sarbis/Veritabani.

Not: *Bu çizelgede depremlerin numaralandırılması, Seyitoğlu vd. (2022a) tarafından deprem kataloğunda listelenen son olay (No. 214) sonrasından, yani 215'ten başlamaktadır. Şekil 3'te gösterilen odak mekanizması çözümleri için 1–214 numaralı olaylar Seyitoğlu vd. (2022a)'ye, 215 ve sonraki numaralı olaylar ise bu çalışmada sunulan verilere karşılık gelmektedir.*

Kısaltmalar: ***Lat.:*** *Enlem****; Lon.:*** *Boylam****; Mag:*** *Magnitude;* ***Str.:*** *Fay doğrultusu (strike);* ***Dip:*** *Eğim (dip);* ***Rake:*** *Kayma açısı;* ***Pazm:*** *Basınç ekseni azimut açısı (pressure azimuth);* ***Pplg:*** *Basınç ekseni dalım açısı (pressure plunge);* ***Tazm:*** *Gerilme ekseni azimut açısı (tension azimuth);* ***Tplg:*** *Gerilme ekseni dalım açısı (tension plunge);* ***Mw:*** *Moment büyüklüğü (moment magnitude);* ***USGS:*** *ABD Jeolojik Araştırmalar Kurumu (U.S. Geological Survey). USA https://earthquake.usgs.gov/earthquakes/search/;* ***KOERI:*** *Boğaziçi Üniversitesi Kandilli Rasathanesi ve Deprem Araştırma Enstitüsü Bölgesel Deprem-Tsunami İzleme Merkezi. http://www.koeri.boun.edu.tr/sismo/zeqdb/ ;* ***AFAD:*** *T.C. İçişleri Bakanlığı Afet ve Acil Durum Yönetimi Başkanlığı. http://www.deprem.gov.tr/sarbis/Veritabani*.

In the hinterland of BZSZ, several rhomboidal cells were described, limited by right- and left-lateral strike-slip faults (Seyitoğlu et al., 2018). In some cases, east-west trending thrusts are located in the middle of the cell (i.e., Van and Ahar rhomboidal cells), which are capable of producing the 2011.10.23 (Mw 7.1) Van earthquake. In other cases, the northern and southern corners of the rhomboidal cells have thrust faults (i.e., Hınıs and Urmiye cells) (Seyitoğlu et al., 2018) (Figure 1).

The rhomboidal cell model in the hinterland of BZSZ contributes to a better understanding of collision-related deformation and helps to define region-wide shear zones, such as the Southeast Anatolian Zagros Fault Zone (SAZFZ). It comprises the southwest margin of Kiğı, Karlıova, Muş, Van and Urmiye cells together with the Main Recent Fault in Iran. This newly-recognised right-lateral shear zone indicates that the NAFZ has a releasing stepover with the SAZFZ, in which the Kiğı, Karlıova and Muş rhomboidal cells developed (Seyitoğlu et al., 2018) (Figure 1).

The rhomboidal cell model (Seyitoğlu et al., 2018) and the Anatolian Diagonal, a broad left-lateral shear zone (Seyitoğlu et al., 2022a), define multiple interaction points between right- and left-lateral faults zones. This is different to the tectonic escape model of Şengör et al. (1985), which suggests a single interaction point.

The first interaction point (#1 in Figure 1) is near Bingöl where the highest strain rates obtained by GNNS data, independent from the structures, are observed in the region (Seyitoğlu et al., 2018; Fig. 10.22B). The SAZFZ cuts the EAFZ, and its previously defined segments between Bingöl and Karlıova (Duman and Emre, 2013) are evaluated as the common margin of the Karlıova and Muş rhomboidal cells. In this case, it can be said that the EAFZ started in Bingöl (Seyitoğlu et al., 2018; 2022a; Fig. 9). This cross-cutting relationship can also be seen in the recently-published tomographic slices of Güvercin (2023; Fig. 6). The EAFZ, the southeast margin of the Anatolian Diagonal, reaches the Cyprus Arc after having two triple junctions with the Dead Sea Fault Zone, which is clearly observed after the earliest releases of surface rupture maps belonging to the recent 2023.02.06 earthquakes (Esat and Seyitoğlu, 2023; Seyitoğlu and Esat, 2023; Özkan et al., 2023; Seyitoğlu et al., 2022a) (TJ-1 and TJ-2 in Figure 1).

The second interaction point (#2 in Figure 1) is west of Tunceli where the left-lateral Ovacık Fault of the Anatolian Diagonal cuts the right-lateral Nazımiye Fault of the SAZFZ. The Ovacık Fault is connected to the Malatya Fault further southwest and several structures such as Sürgü, Barış-Kantarma, Maraş-Yumurtalık, Sarız, and Elbistan-Misis faults accommodate internal deformation of the Anatolian Diagonal (Yusufoğlu, 2013; Acarel et al., 2019; Kaymakçı et al., 2006; Sançar et al., 2020; Seyitoğlu et al., 2022a; Fig. A17 in Appendix A).

The third intersection point (#3 in Figure 1) is located southeast of the Erzincan Plain where the right-lateral NAFZ meets the left-lateral Ovacık Fault of the Anatolian Diagonal. This location, at the same time, constitutes the northern corner of the Kiğı rhomboidal cell (Seyitoğlu et al., 2018; 2022a; Fig. A17).

The fourth intersection point (#4 in Figure 1) is located northwest of the Erzincan Plain where the left-lateral Karaca Fault of the Anatolian Diagonal separates from the right-lateral NAFZ. The semi-parallel left-lateral Karaca Fault and the Kemah-İliç Fault form a restraining bend (i.e., Divriği Thrust) with the Ecemiş-Deliler Fault that constitutes the northwest margin of the Anatolian Diagonal (Seyitoğlu et al., 2022a). This structure reaches the western coast of the Mersin Gulf and its continuation in the Mediterranean Sea, the Biruni Fault, provides a connection to the Cyprus Arc west of Cyprus (Seyitoğlu et al., 2022a and this paper).

The initial definition of the Biruni Fault as an offshore continuation of the Ecemiş-Deliler Fault was based on limited seismic reflection data with poor coordinate system (Seyitoğlu et al., 2022a). In this paper, we provide more reliable coordinate control on the seismic reflection sections obtained from TPAO, more detailed morphological analysis of the onshore continuation around Silifke, and reliable focal mechanism solutions for the earthquakes attributed to the Biruni Fault.

The Biruni Fault's database presented in this paper indicates that the definition of the Kozan Fault zone (Aksu et al., 2014a, b) is doubtful. The Biruni Fault better explains the left-lateral motion between Anatolia and Cyprus because (1) the seismic reflection sections of Aksu et al. (2014a, b) lack solid evidence for a left-lateral fault zone, (2) the position of the Kozan Fault zone, that is distant from the western coast of the Mersin Gulf, cannot explain the southwestern shift of the Göksu River's delta which is better explained by the southwestern end of the EDF lying on the western coast of the Mersin Gulf (Figure 2), and (3) the single and continuous extension of the Kozan Fault zone in the Adana basin and its connection to the EAFZ is unrealistic because the seismic sections of Burton-Ferguson et al. (2005) indicate a restraining stepover south of Adana city between the left-lateral Ecemiş-Deliler and Elbistan-Misis faults of Seyitoğlu et al. (2022a).

When the seismic activity is taken into account, the Ptolemy-Pliny-Strabo Fault Zone is more active relative to the Biruni Fault (Figure 3). This statement is also supported by GNNS-based block modelling, which indicates that the southwest translation of Anatolia is mainly accommodated by the Ptolemy-Pliny-Strabo Fault zone and the Antalya-Kekova Fault Zone where the left-lateral slip rates reach up to 30 mm/yr (Seyitoğlu et al., 2022b). However, the pronounced morphotectonic expression along the Biruni Fault, together with the Pliocene–Quaternary slip rate inferred in this study may indicate a period of higher slip rates during the Quaternary. In contrast, the present-day fault activity, characterised by lower slip rates and reduced seismicity, is consistent with the current lack of significant earthquake activity. As previously noted by Seyitoğlu et al. (2022a), restraining stepovers exist between the Biruni Fault, the Antalya-Kekova Fault Zone, and the Ptolemy-Pliny-Strabo Fault Zone where the Antalya Thrusts, Florence Rise and Fethiye Thrusts developed (Figures 1, 3). This complex relationship is the subject of another paper providing onshore and offshore data from the region.

CONCLUSION

The northwest margin of the Anatolian Diagonal, the Ecemiş-Deliler Fault and its offshore continuation of the Biruni Fault are described in this paper with the help of seismic reflection data from Turkish Petroleum. The position of the

Biruni Fault and the southwest tip of Ecemiş-Deliler Fault better explain the Quaternary shift of the Göksu delta. The focal mechanisms of the recent earthquakes presented in this paper also demonstrate that the Biruni Fault is a left-lateral active structure. Its relationship with the Antalya-Kekova Fault Zone and Ptolemy-Pliny-Strabo Fault Zone implies slip partitioning in the eastern Mediterranean.

GENİŞLETİLMİŞ ÖZET

Anadolu Çaprazı, Doğu Anadolu Fay Zonu ile Orta Anadolu Fay Zonu arasında yer alan, yaklaşık 170 km genişliğinde ve Erzincan'dan Kıbrıs Yayına kadar uzanan 850 km uzunluğunda sol yanal bir makaslama zonu olarak tanımlanmaktadır (Seyitoğlu vd., 2022). Bu zonun güneybatı ucunda bulunan Ecemiş Deliler Fayı'nın güneybatı kesimine ait jeomorfolojik veriler, fayın kuzeydoğu bölümünde belirgin bir doğrusal gidişin hakim olduğunu; buna karşılık güneybatı bölümünde, kıyı şeridine paralel uzanan, KD-GB doğrultulu, sol yanal aralı aşmalı faylardan oluşan ve 20 km'ye ulaşan genişlikte bir makaslama zonu varlığını ortaya koymaktadır. Fay, güneybatı bölümünde KD-GB uzanımlı doğrusal vadiler ile belirgin olup, güncel akarsu yatakları ve Kuvaterner yaşlı morfolojik birimlerde oluşturduğu ötelenmelerle tanımlanmıştır. Bu kesiminde, Göksu Nehri boyunca ölçülen 18 km'lik ötelenme, akarsuyun yaklaşık 8 My önce oluştuğu kabulüyle değerlendirilmiş ve buna dayanarak fayın uzun dönemli ortalama kayma hızı 2,25 mm/yıl olarak hesaplanmıştır.

Anadolu Çaprazı boyunca uzanan sol yanal doğrultu atımlı Ecemiş Deliler Fayı'nın (EDF) denizdeki devamı Biruni Fayı (BRF) olarak tanımlanmıştır. Türkiye Petrolleri Anonim Ortaklığı (TPAO) tarafından sağlanan sismik yansıma kesitlerinde Biruni fayına ait segmentler net bir şekilde izlenmekte ve fayın deniz tabanında meydana getirdiği deformasyonlar takip edilebilmektedir (Şekil 5-14). Kuzeydoğuda, EDF'nin güneybatı ucundan başlayarak güneye doğru takip edilen fay güneyde daralmalı sıçrama yaparak Fuat Sezgin yükselimini oluşturmaktadır (Şekil 9). En güneyde Ptolemy-Pliny-Strabo Fay Zonu ile Biruni Fayı birbirine paralel sol yanal fay sistemler olarak değerlendirilmektedir (Şekil 1,3). Bu faylar arasında, daha önce Akdeniz Sırtı olarak bilinen ve günümüzde Piri Reis Sırtı olarak adlandırılan yapı gelişmiştir (Seyitoğlu vd., 2022a) (Şekil 1, 3).

Çalışma alanı sınırları içerisinde gerçekleşmiş ve moment büyüklüğü 4.5'ten büyük olan depremlerin odak mekanizması çözümleri, güvenilir veri tabanlarından taranmış, ayrıca dış merkezi Biruni fayı üzerinde bulunan iki depremin odak mekanizması çözümleri analiz edilmiştir. (Şekil 15-17 ve Çizelge 1). Biruni Fayı boyunca kaydedilen depremlerin sol yönlü doğrultu atımlı mekanizması ve dağılımı, fayın aktif bir sol yanal fay zonu olduğunu göstermektedir.

ACKNOWLEDGEMENTS

This paper is a part of nearly completed PhD thesis of the first author at Ankara University in the Department of Geological Engineering, Tectonics Research Group supervised by the senior author. We thank the Turkish Petroleum Company for the permission to access and publish offshore data. We are also grateful to two anonymous referees for their valuable comments and to Erdinç Yiğitbaş for editorial handling.

ORCID

Nuray Şahbaz https://orcid.org/0009-0007-2738-2335

Esra Tunçel https://orcid.org/0000-0001-7434-4111

Bülent Kaypak https://orcid.org/0000-0003-4650-9171

Gürol Seyitoğlu https://orcid.org/0000-0001-7993-898X

REFERENCES

Acarel, D., Cambaz M. D., Turhan, F., Kömeç Mutlu A. & Polat, R. (2019). Seismotectonics of Malatya Fault, Eastern Turkey. *Open Geosciences, 11*(1), 1098-11111. https://doi.org/10.1515/geo-2019-0085

Aksu, A. E., Calon, T. J., Hall, J., Mansfield, S. & Yaşar, D. (2005). The Cilicia–Adana basin complex, Eastern Mediterranean: Neogene evolution of an active fore-arc basin in an obliquely convergent margin. *Marine Geology, 221*, 121-159. https://doi.org/10.1016/j.margeo.2005.03.011

Aksu, A. E., Calon, T., Hall, J., Kurtboğan, B., Gürçay, S. & Çiftçi, G. (2014a). Complex interactions fault fans developed in a strike-slip system: Kozan Fault Zone, Eastern Mediterranean Sea. *Marine Geology, 351*, 91-107. https://doi.org/10.1016/j.margeo.2014.03.009

Aksu, A.E., Walsh-Kennedy, S., Hall, J., Hiscott, R. N., Yaltırak, C., Coşkun, S. D. & Çiftçi, G. (2014b). The Pliocene-Quaternary tectonic evolution of the Cilicia and Adana basins, eastern Mediterranean: Special reference to the development of the Kozan Fault zone. *Tectonophysics, 622*, 22-43. https://doi.org/10.1016/j.tecto.2014.03.025

Aksu, A. E., Hall, J. & Yaltırak, C. (2022). The uppermost Messinian-Quaternary evolution of the Anamur-Kormakiti zone: The transition between the outer Cilicia and Antalya basins, northeastern Mediterranean. *Marine and Petroleum Geology, 136*, Article 105451. https://doi.org/10.1016/j.marpetgeo.2021.105451

Aktaş, G. & Robertson, A. H. F. (1984). The Maden complex, SE Turkey: evolution of a Neotethyan active margin. *Geological Society, London, Special Publications, 17*, 375-402. https://doi.org/10.1144/GSL.SP.1984.017.01

Akyüz, H. S., Uçarkuş, G., Altunel, E., Doğan, B. & Dikbaş, A. (2012). Paleoseismological investigations on slow-moving active fault in central Anatolia, Tecer Fault, Sivas. *Annals of Geophysics, 55*, 847-857. https://doi.org/10.4401/ag-5444

Alan, İ., Balcı, V. & Elibol, H. (2014). *Geological map of the Silifke-P31 and P32 Quadrangles*. MTA Ankara, Türkiye.

Anastasakis, G. & Kelling, G. (1991). Tectonic connection of the Hellenic and Cyprus arcs and related geotectonic elements. *Marine Geology, 97*, 261-277. https://doi.org/10.1016/0025-3227(91)90120-S

Arvidsson, R., Avraham, Z. B., Ekström, G. & Wdowinski, S. (1998). Plate tectonic framework for the October 9, 1996, Cyprus earthquake. *Geophysical Research Letters, 25*, 2241-2244. https://doi.org/10.1029/98GL01547

Barrier, E., Chamot-Rooke, N. & Giordano, G. (2004). *Geodynamic Maps of the Mediterranean-sheet 1: Tectonics and Kinematics*. Commission for the Geological map of the World (CGMW) and UNESCO.

Blumental, M. M. (1941). *Niğde ve Adana Vilayetleri dolayındaki Toroslar'ın Jeolojisine umumi bir bakış*. General Directorate for Mineral Research and Exploration (MTA), Publication Series B, no 6, Ankara.

Blumental, M. M. (1952). *Torosların yüksek Aladağ silsilesinin coğrafyası, stratigrafisi ve tektoniği hakkında yeni etüdler*. General Directorate for Mineral Research and Exploration (MTA), Publication Series D, no 6, Ankara.

Burton-Ferguson, R., Aksu, A. E., Calon, T. J. & Hall, J. (2005). Seismic stratigraphy and structural evolution of the Adana basin, eastern Mediterranean. *Marine Geology, 221*, 189-222. https://doi.org/10.1016/j.margeo.2005.03.009

Calon, T. J., Aksu, A. E. & Hall J. (2005). The Oligocene-Recent evolution of the Mesaria Basin (Cyprus) and its western marine extension, Eastern Mediterranean. *Marine Geology, 221*, 95-120. https://doi.org/10.1016/j.margeo.2005.03.012

Cosentino, D., Schildgen, T. F., Cipollari, P., Faranda, C., Gliozzi, E., Hudackova, N., Lucifora, S. & Strecker, M. R. (2012). Late Miocene surface uplift of the southern margin of the Central Anatolian Plateau, Central Taurides, Turkey. *Geological Society of America Bulletin, 124*(1-2), 133-145. https://doi.org/10.1130/B30466.1

Darin, M. & Umhoefer, P. (2019). Structure and kinematic evolution of the southern Sivas fold-thrust belt, Sivas Basin, Central Anatolia, Turkey. *Turkish Journal of Earth Sciences, 28*(6), 834-859. https://doi.org/10.3906/yer-1907-29

Dewey, J. F., Hempton, M. R., Kidd, W. S. F., Şaroğlu, F. & Şengör, A. M. C. (1986). Shortening of continental lithosphere: the neotectonics of Eastern Anatolia a young collision zone. In:

Coward MP, Ries AC, (ed). Collision Tectonics. *Geological Society London Special Publications, 19*, 3-36 (Robert M. Shackleton volume). https://doi.org/10.1144/gsl.sp.1986.019.01.01

Dirik, K. (2001). Neotectonic evolution of the northwestward arched segment of the Central Anatolian Fault Zone, Central Anatolia, Turkey. *Geodinamica Acta, 14*, 147-158. https://doi.org/10.1016/S0985-3111(00)01056-1

Dirik, K. & Göncüoğlu, M. C. (1996). Neotectonic Characteristics of Central Anatolia. *International Geology Review, 38*, 807-817. https://doi.org/10.1080/00206819709465363

Duman, T. & Emre, Ö. (2013). The East Anatolian Fault: geometry, segmentation and jog characteristics. *Geological Society, London, Special Publications, 372*, 495-529. https://doi.org/10.1144/SP372.14

Elmacı, H., Gürboğa, Ş., Özalp, S., Avcı, H. O., Aydoğan, H., Yavuzoğlu, A., Yüce, A. A., Kara, M. & Öztürker, A. R. (2025). Active tectonic characteristics of the Turkish Republic of Northern Cyprus in light of paleoseismological data. Şen, C. & Bak, T. (Eds.), *77th Geological Congress of Türkiye, Abstract Book* (p.: 343). Chamber of Geological Engineers of Türkiye Publications. https://www.jmo.org.tr/resimler/ekler/662575e8a4e2055_ek.pdf

Emre, Ö., Duman, T., Özalp, S., Elmacı, H., Olgun, Ş. & Şaroğlu, F. (2013). *Active fault map of Turkey with and explanatory text*. Special Publication Series 30. General Directorate of Mineral Research and Exploration (MTA). ISBN: 978-605-5310-56-1

Esat, K. & Seyitoğlu, G. (2023). *Surface rupture map of the 2023.02.06 Kahramanmaraş Earthquakes based on high-resolution satellite and aerial imagery*. ResearchGate Technical Report. https://doi.org/10.13140/RG.2.2.36259.32808

Evans, G., Morgan, P., Evans, W. E., Evans, T. R. & Woodside, J. M. (1978). Faulting and halokinetics in the northeastern *Mediterranean between Cyprus and Turkey. Geology, 6,* 392-396. https://doi.org/10.1130/0091-7613(1978)6<392:FAHITN>2.0.CO;2

Güneş, P., Aksu, A. E. & Hall, J. (2018). Structural framework and deformation history of the western Cyprus Arc. *Tectonophysics, 744*, 438-457. https://doi.org/10.1016/j.tecto.2018.07.023

Güvercin, S.E. (2023). A local earthquake tomography on the EAFZ shows dipping fault structure. *Turkish Journal of Earth Sciences, 32*(3): 294-305. https://doi.org/10.55730/1300-0985.1845

Hall, R. (1976). Ophiolite emplacement and the evolution of the Taurus suture zone, southeast Turkey. *Geological Society of America, 87*, 1078-1088.

Herrmann, R. B. (2013). Computer programs in seismology: An evolving tool for instruction and research. *Seismological Research Letters, 84*, 1081-1088. https://doi.org/10.1785/0220110096

Higgins, M., Schoenbohm, L. M., Brocard, G., Kaymakçı, N., Gosse, J. C. & Cosca, M. A. (2015). New kinematic and geochronologic evidence for the Quaternary evolution of the Central Anatolian fault zone (CAFZ). *Tectonics, 34*, 2118-2141. https://doi.org/10.1002/2015TC003864

Huguen, C., Mascle, J., Chaumillon, E., Woodside, J. M., Benkhelil, J. Kopf, A. & Volkonskaia, A. (2001). Deformational styles of the eastern Mediterranean Ridge and surroundings from combined swath mapping and seismic reflection profiling. *Tectonophysics, 343*, 21-47. https://doi.org/10.1016/S0040-1951(01)00185-8

İnan, S. ve Ekingen, S. (2007). Namrun Fay Zonu'nun jeolojik – morfotektonik özellikleri: Orta Anadolu Fay Sistemi'nin güneybatı bölümü (Orta Toroslar – Türkiye). *Yerbilimleri, 28*, 147-158.

Jaffey, N. & Robertson, A. H. F. (2001). New sedimentological and structural data from the Ecemiş Fault Zone, southern Turkey: implications for its timing and offset and the Cenozoic tectonic escape of Anatolia. *Journal of the Geological Society, London, 158, 367-378*. https://doi.org/10.1144/jgs.158.2.367

Kaymakçı, N., İnceöz, M. & Ertepınar, P. (2006). 3d-Architecture and Neogene evolution of the Malatya basin: Inferences for the kinematics of the Malatya and Ovacık fault zones. *Turkish Journal of Earth Sciences, 15*, 123-154.

Ketin, İ. (1960). Tectonic units of Anatolia. *Bulletin of the Mineral Research and Exploration (MTA), 54*, 20-34.

Koçyiğit, A. & Beyhan, A. (1998). A new intracontinental transcurrent structure: The Central Anatolian Fault Zone, Turkey. *Tectonophysics, 284*, 317-336. https://doi.org/10.1016/S0040-1951(97)00176-5

Kuzucuoğlu, C., Çiner, A. & Kazancı, N. (2019). The geomorphological regions of Turkey. In

Kuzucuoğlu, C., Çiner, A. & Kazancı, N (Eds.), *Landscapes and Landforms of Turkey*, (p.: 41-178). World Geomorphological Landscapes. Springer, Cham. https://doi.org/10.1007/978-3-030-03515-0_4

Mansfield, S. L. (2005). *Neogene Tectonic and Sedimentary Evolution of the Outer Cilicia Basin, Eastern Mediterranean Sea* [MSc Thesis]. Memorial University of Newfoundland and Labrador. ISBN: 978-0-494-19380-8.

McKenzie, D. P. (1972). Active tectonics of the Mediterranean region. *Geophysical Journal International, 30*, 109-185. https://doi.org/10.1111/j.1365-246X.1972.tb02351.x

Metz, K. (1956). Aladağ ve Karanfil Dağı'nın yapısı ve bunların Kilikya Torosu tesmiye edilen batı kenarları hakkında malümat husulü için yapılan jeolojik etüt. *Bulletin of Mineral Research and Exploration (MTA), 48*, 63-76.

Özel, E., Uluğ, A. & Pekçetinöz, B. (2007). Neotectonic aspects of the northern margin of the Adana-Cilicia submarine basin, NE Mediterranean. *Journal of Earth System Science, 116*(2), 113-124. https://doi.org/10.1007/s12040-007-0011-9

Özkan, A., Yavaşoğlu, H. H. & Masson, F. (2023). Present-day strain accumulations and fault kinematics at the Hatay Triple Junction using new geodetic constraints. *Tectonophysics, 854*, Article 229819. https://doi.org/10.1016/j.tecto.2023.229819

Pavoni, N. (1961). Die Nordanatolische Horizontalverschiebung. *Geologische Rundschau, 51*, 122-139.

Pilidou, S., Priestley, K., Jackson, J. & Maggi, A. (2004). The 1996 Cyprus earthquake: a large, deep event in the Cyprean Arc. *Geophysical Journal International, 158*, 85-97. https://doi.org/10.1111/j.1365-246X.2004.02248.x

Reilinger, R., McClusky, S., Vernant, P., Lawrence, S., Ergintav, S., … & Karam, G. (2006). GPS constraints on continental deformation in the Africa - Arabia-Eurasia continental collision zone and implications for the dynamics of plate interactions. *Journal of Geophysical Research, 111*, Article B05411. https://doi.org/10.1029 / 2005JB004051

Sançar, T., Zabcı, C., Akçar, N., Karabacak, V., Yeşilyurt, S., Yazıcı, M., Akyüz, H.S., Öztüfekçi Önal, A., Ivy-Ochs, S., Christl, M. & Vockenhuber, C. (2020). Geodynamic importance of the strike-slip faults at the eastern part of the Anatolian Scholle: Inferences from the uplift ond slip rate of the Malatya Fault (Malatya-Ovacık Fault Zone, eastern Turkey). *Journal of Asian Earth Sciences, 188*, Article 104091. https://doi.org/10.1016/j.jseaes.2019.104091

Sarıkaya, M. A., Yıldırım, C. & Çiner, A. (2015a). No surface breaking on the Ecemiş Fault, central Turkey, since Late Pleistocene (~64.5ka); new geomorphic and geochronologic data from cosmogenic dating of offset alluvial fans. *Tectonophysics, 649*, 33-46. https://doi.org/10.1016/j.tecto.2015.02.022

Sarıkaya, M.A., Yıldırım, C. & Çiner, A. (2015b). Late Quaternary alluvial fans of Emli Valley in the Ecemiş Fault Zone, south central Turkey: Insights from cosmogenic nuclides. *Geomorphology, 228*, 512-525. https://doi.org/10.1016/j.geomorph.2014.10.008

Schildgen, T. F., Cosentino, D., Bookhagen, B., Niedermann, S., Yıldırım, C., Echtler, H., Wittmann, H. & Strecker, M.R. (2012). Multi-phased uplift of the southern margin of the Central Anatolian plateau, Turkey: A record of tectonic and upper mantle processes. *Earth and Planetary Science Letters, 317-318*, 85-95. https://doi.org/10.1016/j.epsl.2011.12.003

Scott, B. (1981). The Eurasian-Arabian and African continental margin from Iran to Greece. *Journal of Geological Society, London, 138*, 7694-7706.

Seyitoğlu, G., Esat, K. & Kaypak, B. (2017). The neotectonics of southeast Turkey, northern Syria and Iraq: the internal structure of the South East Anatolian Wedge and its relationship with the recent earthquakes. *Turkish Journal of Earth Sciences, 26*, 105-126. https://doi.org/10.3906/yer-1605-21

Seyitoğlu, G., Esat, K., Kaypak, B., Toori, M. & Aktuğ, B. (2018). Internal deformation of the Turkish-Iranian Plateau in the hinterland of Bitlis-Zagros Suture Zone. In Farzipour Saein A. (Ed), *Tectonic and Structural Framework of the Zagros Fold-Thrust Belt* (pp.: 161-244). Developments in Structural Geology and Tectonics Volume 3. Elsevier. https://doi.org/10.1016/B978-0-12-815048-1.00010-X

Seyitoğlu, G., Tunçel, E., Kaypak, B., Esat, K. & Gökkaya, E. (2022a). The Anatolian Diagonal: A

left lateral shear zone between East and Central Anatolia and its relationship with both North Anatolian Fault Zone and Aegean Cyprus Arcs. *Geological Bulletin of Turkey, 65*(2), 93-116. https://doi.org/10.25288/tjb.1015537

Seyitoğlu, G., Aktuğ, B., Esat, K. & Kaypak, B. (2022b). Neotectonics of Turkey (Türkiye) and surrounding regions: a new perspective with block modelling. *Geologica Acta, 20*, 1-21. https://orcid.org/0000-0001-7993-898X

Seyitoğlu, G., Esat, K., Kaypak, B. & Koca, B. (2022c). Seismotectonics of the southern branch of North Anatolian Fault Zone along Bolu, Bursa, and İzmir cities and Değirmenlik (Milos) island in the Aegean Sea. *Yerbilimleri-Bulletin for Earth Sciences, 43*(2), 138-159. https://doi.org/10.17824/yerbilimleri.948130

Seyitoğlu, G. & Esat, K. (2023). Structural relationship between the Dead Sea Fault Zone and East Anatolian Fault Zone: The cross-basin Kadıncık Fault emerged by the 2023.02.06 Kahramanmaraş (M=7.8) earthquake's surface rupture. In Bozkurt, E., Dumanlılar, Ö., Akyıldız, M., Yılmaz, K. K., Coşkun Tunaboylu, B., Cihan, Z. Ö., Yağbasan, Ö. & Şükran Açıkel (Eds.), *75th Geological Congress of Türkiye*, *Abstract Book* (p.: 94). Chamber of Geological Engineers of Türkiye Publications. https://www.jmo.org.tr/resimler/ekler/24f25904af8a59f_ek.pdf

Symeou, V., Homberg, C., Nader, F.H., Darnault, R., Lecomte, J-C., & Papadimitriou, N. (2018). Longitudinal and temporal evolution of the tectonic style along the Cyprus Arc system, assessed through 2-D reflection seismic interpretation. *Tectonics, 37*, 30-47. https://doi.org/10.1002/2017TC004667

Şaroğlu, F., Emre, Ö. & Kuşçu, İ. (1992). *Active Fault Map of Turkey. Ankara, Turkey*. General Directorate of Mineral Research and Exploration (MTA).

Şengör, A. M. C. (1979). The North Anatolian transform fault: its age, offset and tectonic significance. *Journal of the Geological Society, 136*, 269-282. https://doi.org/10.1144/gsjgs.136.3.0269

Şengör, A. M. C. & Kidd, W. S. F. (1979). Post-collisional tectonics of the Turkish-Iranian Plateau and a comparison with Tibet. *Tectonophysics, 55*, 361-376. https://doi.org/10.1016/0040-1951(79)90184-7

Şengör, A. M. C. (1980). *Türkiye'nin Neotektoniğinin Esasları [Fundamentals of the Neotectonics of Turkey]*. Publication of Geological Society of Turkey, 1-40.

Şengör, A. M. C., & Yılmaz, Y. (1981). Tethyan evolution of Turkey: A plate tectonic approach. *Tectonophysics, 75*, 181-241. https://doi.org/10.1016/0040-1951(81)90275-4

Şengör, A. M. C., Görür, N. & Şaroğlu, F. (1985). Strike-slip deformation basin formation and sedimentation: Strike-slip faulting and related basin formation in zones of tectonic escape: Turkey as a case study. In Biddle, K.T., Christie-Blick, N., (Eds.), *Strike-slip faulting and basin formation*. *Society of Economic Paleontologists and Mineralogists, 37*, 227-264. https://doi.org/10.2110/pec.85.37

Şengör, A. M. C., Özeren, S., Genç, T. & Zor, E. (2003). East Anatolian high plateau as a mantle-supported, north-south shortened domal structure. *Geophysical Research Letters, 30*(24) Article 8045. https://doi.org/10.1029/2003GL017858

Şengör, A. M. C., Özeren, M. S., Keskin, M., Sakınç, M., Özbakır, A. D. & Kayan, İ. (2008). Eastern Turkish high plateau as a small Turkic-type orogen: Implications for post-collisional crust-forming processes in Turkic-type orogens. *Earth-Science Reviews, 90*(1), 1-48. https://doi.org/10.1016/j.earscirev.2008.05.002

Şengör, A. M. C. (2017). Diversion of River Courses Across Major Strike-Slip Faults and Keirogens. In Çemen, İ. & Yılmaz, Y. (Eds.), *Active Global Seismology: Neotectonics and Earthquake Potential of the Eastern Mediterranean Region* (pp.: 93-101). Geophysical Monograph Series, 225. https://doi.org/10.1002/9781118944998.ch3

Şengör, A. M. C., Zabcı, C. & Natal'in, B. A. (2019). Continental Transform Faults: Congruence and Incongruence with normal plate kinematics. In Duarte, J. C, (Ed.), *Transform Plate Boundaries and Fracture Zones* (pp.: 169-247) Elsevier. https://doi.org/10.1016/B978-0-12-812064-4.00009-8

Tatar, O., Piper, J. D. A. & Gürsoy, H. (2000). Palaeomagnetic study of the Erciyes sector of the Ecemiş Fault Zone: neotectonic deformation in the southeastern part of the Anatolian Block. In: Tectonics and Magmatism in Turkey and the Surrounding Area. *Geological Society, London,*

Special Publications, 173, 423-440. https://doi.org/10.1144/gsl.sp.2000.173.01.20

Woodside, J.M., Mascle, J., Zitter, T.A.C., Limonov, A.F., Ergün, M., Volkonskaia, A. & shipboard scientist of the PRISMED II Expedition. (2002). The Florence Rise, the western bend of the Cyprus Arc. *Marine Geology, 185*, 177-194. https://doi.org/10.1016/S0025-3227(02)00194-9

Yetiş, C. (1978). *Çamardı (Niğde ili) yakın ve uzak dolayının jeoloji incelemesi ve Ecemiş yarılım kuşağının Maden Boğazı – Kamışlı arasındaki özellikleri* [Doktora Tezi]. İstanbul Üniversitesi Fen Fakültesi, 151s.

Yıldırım, C., Sarıkaya, M. A. & Çiner, A. (2016). Late Pleistocene intraplate extension of the Central Anatolian Plateau, Turkey: Inferences from cosmogenic exposure dating of alluvial fan, landslide, and moraine surfaces along the Ecemiş Fault Zone. *Tectonics, 35*, 1446-1464. https://doi.org/10.1002/2015TC004038

Yılmaz, Y. (1993). New evidence and model on the evolution of the southeast Anatolian orogen. *Geological Society of America Bulletin, 105*(2), 251-271. https://doi.org/10.1130/0016-7606(1993)105<0251:NEAMOT>2.3.CO;2

Yusufoğlu, H. (2013). An intramontane pull-apart basin in tectonic escape deformation: Elbistan Basin, Eastern Taurides, Turkey. *Journal of Geodynamics, 65*, 308-329, https://doi.org/10.1016/j.jog.2012.05.012